



# A robust heterodimeric Fc platform engineered for efficient development of bispecific antibodies of multiple formats

Gregory L. Moore<sup>\*,1</sup>, Matthew J. Bernett<sup>\*,1</sup>, Rumana Rashid, Erik W. Pong, Duc-Hanh T. Nguyen, Jonathan Jacinto, Araz Eivazi, Alex Nisthal, Juan E. Diaz, Seung Y. Chu, Umesh S. Muchhal, John R. Desjarlais

Xencor, Inc., Monrovia, CA, United States

## ARTICLE INFO

### Keywords:

Bispecific antibody  
Heterodimeric Fc  
Fc engineering  
Tumor-associated antigen × CD3  
Developability

## ABSTRACT

Bispecific monoclonal antibodies can bind two protein targets simultaneously and enable therapeutic modalities inaccessible by traditional mAbs. Bispecific formats containing a heterodimeric Fc region are of particular interest, as a heterodimeric Fc empowers both bispecificity and altered valencies while retaining the developability and druggability of a monoclonal antibody. We present a robust heterodimeric Fc platform, called the XmAb<sup>®</sup> bispecific platform, engineered for efficient development of bispecific antibodies and Fc fusions of multiple formats. First, we engineer a purification solution for proteins containing a heterodimeric Fc using engineered isoelectric point differences in the Fc region that enable straightforward purification of the heterodimeric species. Then, we combine this purification solution with a novel set of Fc substitutions capable of achieving heterodimer yields over 95% with little change in thermostability. Next, we illustrate the flexibility of our heterodimeric Fc with a case study in which a wide range of tumor-associated antigen × CD3 bispecifics are generated, differing in choice of tumor antigen, affinities for both tumor antigen and CD3, and tumor antigen valency. Finally, we present manufacturing data reinforcing the robustness of the heterodimeric Fc platform at scale.

## 1. Introduction

Monoclonal antibodies (mAbs) have become a large and important class of therapeutics and there are currently over seventy antibody-based drugs that are marketed or pending approval [1]. Bispecific monoclonal antibodies (bispecifics), enabled by recent technology in protein engineering, have emerged as a growing new class of therapeutics. These antibodies, as their name suggests, can bind two protein targets simultaneously and allow therapeutic modalities inaccessible by traditional mAbs. Some of these newly enabled functions include recruiting immune cells to tumors for more effective treatment of cancer, dual-blocking of receptors for more effective inhibition of autoimmune activity, and even accurately positioning two separate enzymes to mimic cofactor activity [2,3]. Only two bispecific antibodies are currently approved and marketed (blinatumomab [4], targeting CD19 and

CD3, and emicizumab [3], targeting coagulation factors IXa and X). However, a recent snapshot of company pipelines from the Tabs Therapeutic Antibody Database [5] lists 56 bispecifics out of a total of 822 antibodies (7%) with Phase 1 through Phase 3 status. When only Phase 1 antibodies are examined, this percentage increases to 11% (34 out of 313), indicating a rapidly growing interest in testing bispecifics and their novel therapeutic modalities.

A vast array of bispecific formats have been suggested [2]. We have been particularly interested in formats containing a heterodimeric Fc region as it empowers both bispecificity and altered valencies while retaining the developability and druggability of a mAb (e.g., protein A binding for production, FcRn binding for half-life, effector function when desired). Some examples of “1 + 1” and “2 + 1” mixed-valency bispecifics enabled by a heterodimeric Fc are illustrated in Fig. 1. A heterodimeric Fc also enables many useful classes of Fc fusions,

*Abbreviations:* pI, isoelectric point; mAb, monoclonal antibody; TAA, tumor-associated antigen;  $t_{elution}$ , elution time; IEX, ion exchange; CEC, cation exchange chromatography; AEC, anion exchange chromatography; SEC, size exclusion chromatography; RTCC, redirected T cell cytotoxicity; PQ, product quality; HCP, host cell protein; FcRn, neonatal Fc receptor; SPR, surface plasmon resonance; DSC, differential scanning calorimetry; DSF, differential scanning fluorimetry; LDH, lactate dehydrogenase; ALL, acute lymphoblastic leukemia; HCP, host cell protein; GMP, good manufacturing practice; CRO, contract research organization

\* Corresponding authors.

E-mail addresses: [gmoore@xencor.com](mailto:gmoore@xencor.com) (G.L. Moore), [mbernett@xencor.com](mailto:mbernett@xencor.com) (M.J. Bernett).

<sup>1</sup> These authors contributed equally to this work.

<https://doi.org/10.1016/j.ymeth.2018.10.006>

Received 31 July 2018; Received in revised form 5 October 2018; Accepted 11 October 2018

Available online 23 October 2018

1046-2023/ © 2018 The Authors. Published by Elsevier Inc. This is an open access article under the CC BY-NC-ND license (<http://creativecommons.org/licenses/by-nc-nd/4.0/>).

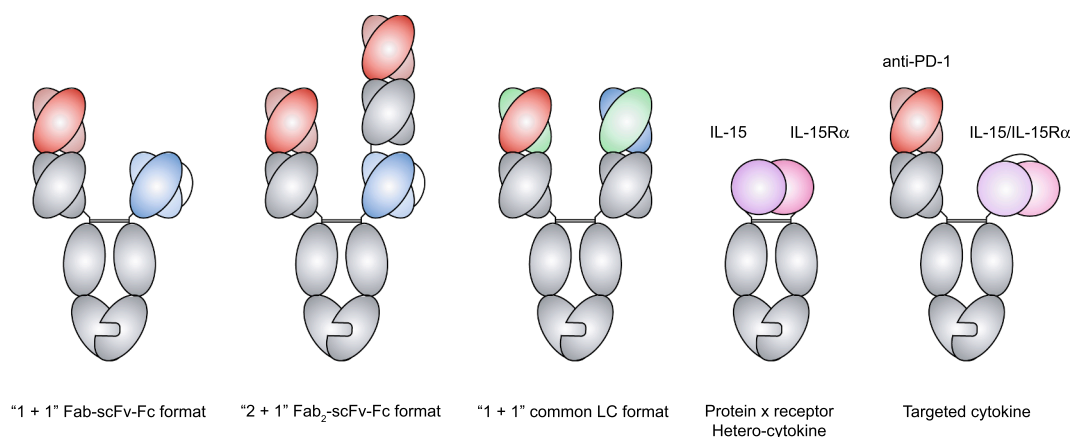


**Fig. 1.** Examples of bispecific antibody, hetero-cytokine, and targeted cytokine formats enabled by heterodimeric Fc technology.

including heterodimeric cytokine/receptor fusions and targeted cytokine formats (Fig. 1). Design of a heterodimeric Fc can be stated as the design of two complementary CH3 domains that show a strong preference for pairing with each other versus pairing with themselves, resulting in a significantly higher yield of heterodimer versus homodimeric or monomeric side products. Pioneering work by Carter and colleagues [6–8] identified “knob-into-hole” approaches successful in promoting heterodimer formation at yields over 85%. This approach used Fc engineering to introduce complementarity at the CH3-CH3 interface by inserting a “knob” (increased side-chain volume) on a first Fc chain while adding a matching “hole” (decreased side-chain volume) on a second Fc chain. Other early approaches to Fc heterodimerization introduced complementarity in different manners, either by charge inversions (electrostatic steering) [9] or multiple IgA substitutions (strand-exchange engineered domain, or SEEDbody) [10]. These “first-generation” approaches were successful in promoting heterodimer formation at relative yields over 85%; however, the thermostabilities of their heterodimeric CH3 regions were reduced compared to those of IgG isotypes commonly used as therapeutic scaffolds (native IgG1  $T_m = 83^\circ\text{C}$ , IgG2  $T_m = 81^\circ\text{C}$ , and IgG4  $T_m = 72^\circ\text{C}$  [11]). Our own first-generation efforts to generate a heterodimeric Fc resulted in an IgG1 variant capable of promoting heterodimer formation at yields up to 89% [12]. However, like the other first-generation approaches, the thermostability of our heterodimeric CH3 ( $T_m = 69^\circ\text{C}$ ) was significantly reduced. This result motivated us to improve on our initial design with the goal of increasing both the relative yield of the heterodimer and the thermostability of the CH3 domain.

Even with the many published solutions to heterodimeric Fc engineering (for a recent review, see Ref. [13]), it is unrealistic to expect any solution to produce completely pure heterodimer, especially at manufacturing scale; and small amounts of homodimeric side products will always need to be removed during production. Various groups have taken different approaches to heterodimer purification. A method utilized by several groups [14–17] is to engineer differential binding to protein A, which allows selective pH elution of the heterodimer during the standard protein A chromatographic step. Other groups have taken an analogous approach with ion exchange (IEX) chromatography by utilizing native or engineered isoelectric point (pI) differences to enable separation [18–20]. However, it is unclear if these approaches will be efficient at manufacturing scale for multiple programs. We sought a “one-size-fits-all” purification solution for heterodimeric Fc using engineered isoelectric point differences in the Fc region that would enable industry-standard IEX purification of the heterodimeric species independent of the Fv regions and format.

In this paper, we present a robust heterodimeric Fc, called the XmAb® bispecific platform, engineered for efficient development of bispecific antibodies and Fc fusions of multiple formats. First, we

engineer a purification solution for proteins containing a heterodimeric Fc using engineered isoelectric point differences in the Fc region that enable straightforward purification of the heterodimeric species. Then, we combine this purification solution with a novel set of Fc substitutions capable of achieving heterodimer yields over 95% while only slightly decreasing the thermostability of the CH2 and CH3 regions. Next, we illustrate the flexibility of our heterodimeric Fc with a case study in which a wide range of tumor-associated antigen (TAA) × CD3 bispecifics are generated differing in tumor-associated antigen, affinities for both tumor-associated antigen and CD3, and tumor-associated antigen valency. Finally, we present manufacturing data reinforcing the robustness of the platform at scale.

## 2. Material and methods

### 2.1. Construction, expression, and purification

Fc-only constructs consisted of native human IgG1 positions 216 through 447 with a C220S substitution to remove the cysteine that typically pairs with a light chain. DNA encoding a standard signal peptide and positions 216 through 236 was generated by gene synthesis (Blue Heron Biotech) and was subcloned into the expression vector pTT5 [21] (National Research Council Canada, Ottawa, Ontario) encoding a native human heavy chain IgG1 Fc region. Substitutions in the Fc domain were introduced using site-directed mutagenesis (Quik-Change, Stratagene, Cedar Creek, TX). Positions are numbered according to the EU index [22].

Fab-scFv-Fc and Fab<sub>2</sub>-scFv-Fc bispecific constructs consisted of three chains: a standard antibody heavy chain, a standard antibody light chain, and either an scFv Fc-fusion or Fab-scFv Fc-fusion chain. Variable regions and scFvs (VH-(GKPGS)<sub>4</sub>-VL) were generated by gene synthesis. For antibody heavy chains, VH regions were subcloned into pTT5 encoding a native human heavy chain IgG1 Fc region; for antibody light chains, VL regions were subcloned into pTT5 encoding either native human light chain C $\kappa$  or C $\lambda$  constant region. For scFv-Fc constructs, scFv regions were subcloned into pTT5 encoding a native human heavy chain IgG1 Fc region; the resulting fusions consisted of native human IgG1 positions 216 through 447. For Fab-scFv-Fc constructs, VH regions (for Fab) and scFv regions were subcloned into pTT5 encoding a native human heavy chain IgG1 Fc region sequentially; the resulting fusions utilized ten amino acid (G<sub>4</sub>S)<sub>2</sub> linkers for the Fab-scFv and scFv-Fc connections and consisted of native human IgG1 positions 222 through 447. The scFv-Fc constructs included a C220S substitution to remove the cysteine that typically pairs with a light chain. Substitutions in the Fc domain were introduced using site-directed mutagenesis.

For protein production, plasmids encoding all necessary protein

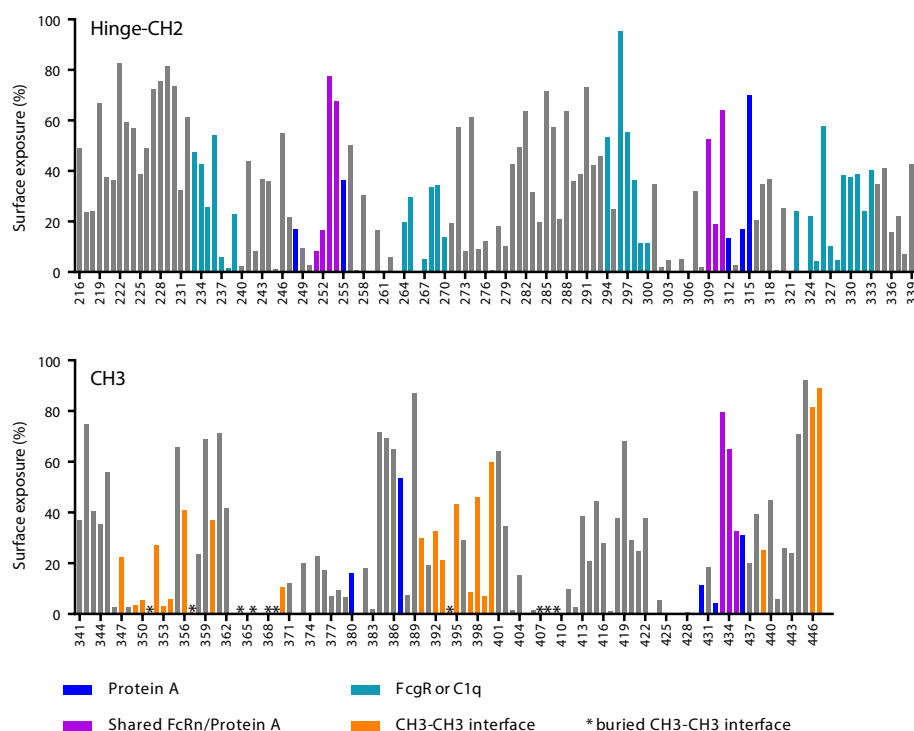


**Fig. 2.** IgG1 hinge, CH2, and CH3 surface exposure and receptor/CH3-CH3 interfaces determined from analysis of several IgG1-receptor complex structures.

chains were co-transfected into HEK293E cells (National Research Council Canada) using 293fectin™ (Invitrogen). Media were harvested five days after transfection, and protein was purified from the supernatant using protein A affinity chromatography (GE Healthcare Life Sciences). For heterodimeric constructs, protein from the protein A step was further purified using either anion exchange chromatography (AEC) or cation exchange chromatography (CEC). For AEC purification, protein was injected onto a HiTrap Q HP 16 × 25 mm (5.0 mL) column (GE Healthcare Life Sciences) at 0.5 mL/min and eluted at 3 mL/min using 50 mM Tris, pH 8.5 as the mobile phase and 50 mM Tris, pH 8.5 plus 1 M NaCl as the elution phase. For CEC purification, protein was injected onto a HiTrap SP HP 16 × 25 mm (5.0 mL) column (GE Healthcare Life Sciences) at 0.5 mL/min and eluted at 2 mL/min using 50 mM MES, pH 6.0 as the mobile phase and 50 mM MES, pH 6.0 plus 1 M NaCl as the elution phase. For both AEC and CEC purification, a linear gradient from 5% to 40% of the elution phase over 12 column volumes was used.

## 2.2. Protein analysis

Proteins were characterized by analytical-scale SEC and either analytical-scale AEC or CEC using an Agilent 1200 HPLC system, which has a lower limit of detection of approximately 0.04 mAU or 5 µg/mL. In the case of an analysis of a protein at 1 mg/mL, this translates to 0.5%. For SEC, proteins were injected onto a Superdex 200 Increase 10/300 GL column (GE Healthcare Life Sciences) at either 0.5 (Fig. 8F) or 1 mL/min (Fig. 8B) using PBS, pH 7.4 as the mobile phase. SEC was coupled with multi-angle light scattering (MALS) (Wyatt Technology Corporation, Goleta, CA) to determine the absolute molecular weights of the proteins in Fig. 8B. For AEC, proteins were injected onto a Proteomix SAX-NP5 column (Sepax Technologies Inc., Newark, DE) at 1 mL/min using 20 mM Tris, pH 8.5 as the mobile phase and 20 mM Tris, pH 8.5 plus 1 M NaCl as the elution phase; a linear gradient from 0% to 40% of the elution phase over 15 min was used. For CEC, proteins were injected onto a ProPac WCX-10 column (ThermoFisher Scientific) at 0.5 mL/min using 20 mM MES, pH 6.0 as the mobile phase and 20 mM MES, pH 6.0 plus 1 M NaCl as the elution phase; a linear

gradient from 0% to 40% of the elution phase over 10 column volumes was used.

## 2.3. Structural analysis and modeling

Crystal structures of an intact full-length IgG mAb (PDB code 1HZH [23]) as well as the Fc region in complex with Fcγ receptors (PDB codes 4W4O [24], 3RY6 [25], 3WJJ [26], 3SGK [27], 1T83 [28]), FcRn (PDB code 4NOU [29]), and Protein A (PDB code 1FC2 [30]) were analyzed for CH3-CH3 interface interactions, Fc receptor contacts, and surface exposure using MOE [31]. For C1q, the electron microscopy structure PDB code 6FCZ [32] was used and analyzed in a similar way. For modeling, a crystal structure of native human IgG1 Fc region (PDB 3AVE [33]) was read into MOE [31]. The QuickPrep tool was used to refine the structure with default settings, which included corrections of structural errors, addition of hydrogens, calculation of partial charges, 3-D optimization of H-bond network (Protonate3D), deletion of water molecules, and a restrained minimization. Amino acid substitutions were made using the Protein Builder module and refined using the module's minimization procedure.

## 2.4. pI calculations

Theoretical protein pI was calculated based on protein sequence using the oscillating method [34]. pKa values of ionizable amino acid side chains were as described in Bjellqvist et al. [35] with no modification for presence on the N- or C-terminus. pKa values for the N-terminal amino group and C-terminal carboxyl group were as described in Refs. [34,35], respectively.

## 2.5. Determination of Fcγ receptor binding

Binding to Fcγ receptors (FcγR) was measured by surface plasmon resonance (SPR) using a Biacore 3000 instrument (GE Healthcare Life Sciences). A protein A sensor chip/antibody capture format with receptor as analyte was used as described previously [36].

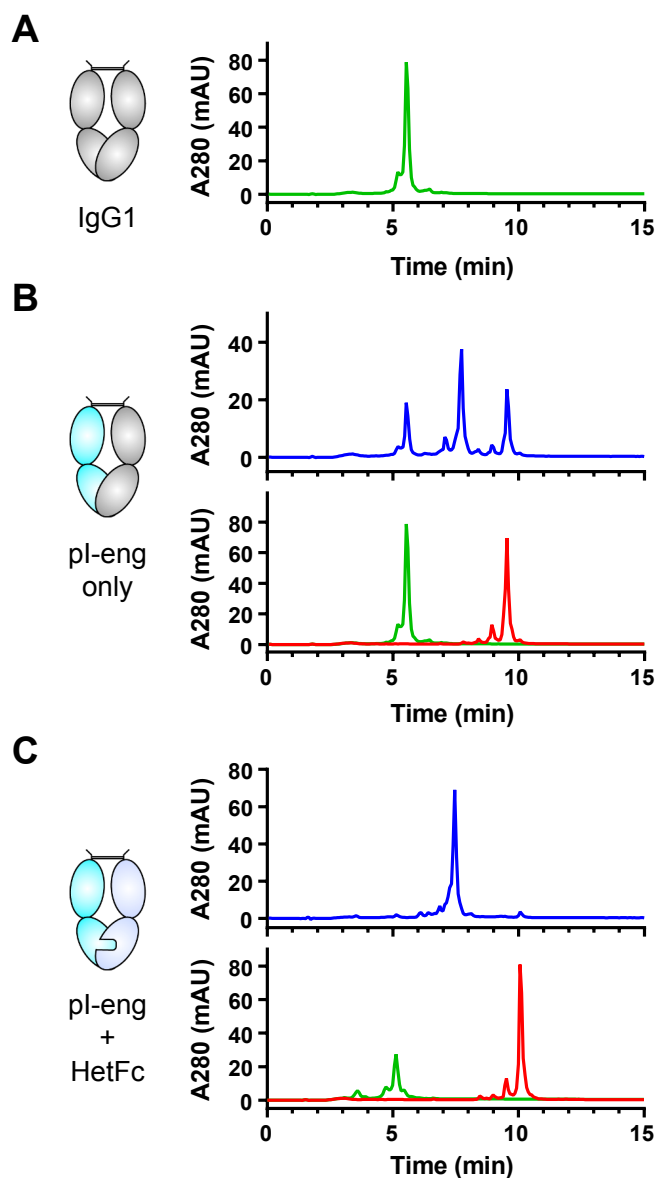


**Fig. 3.** Analytical anion exchange of native IgG1, pI engineered (pI-eng), and pI-eng + heterodimeric Fc (HetFc) engineered Fc-only constructs illustrates the impact of pI engineering on separation of a heterodimer species from homodimer side products as well as the impact of CH3-CH3 HetFc engineering on maximizing the percentage of heterodimer formed. (A) Native IgG1 Fc homodimer ( $pI = 7.3$ ) for reference. (B) *Top*, the three species produced when the pI-reduced Fc-chain is transfected with a native IgG1 Fc-chain include a native IgG1 homodimer species ( $pI = 7.3$ ), a (-/native) heterodimer species ( $pI = 6.4$ ), and a (-/-) homodimer species ( $pI = 6.0$ ) produced at approximately a 25%: 50%: 25% distribution. *Bottom*, separately transfected native IgG1 and (-/-) homodimer species overlaid on the same graph for reference. (C) *Top*, > 95% heterodimer species is produced when pI-reduced L368D/K370S Fc-chain is transfected with S364K/E357Q Fc-chain. *Bottom*, separately transfected pI-reduced S364K/E357Q Fc-chain homodimer ( $t_{elution} = 3.5$  min) and monomer ( $t_{elution} = 5.1$  min), and L368D/K370S Fc-chain homodimer ( $t_{elution} = 10.1$  min) species overlaid on the same graph for reference.

## 2.6. Thermal denaturation measurements

Differential scanning calorimetry (DSC) thermal denaturation experiments were performed using a MicroCal VP-DSC MicroCalorimeter (Malvern Panalytical Inc., Westborough, MA). Proteins were diluted to 0.25 mg/mL (Fc-only) or 0.5 mg/mL (bispecifics) in PBS and degassed. Degassed proteins were heated from 25 to 100 °C using a heating rate of

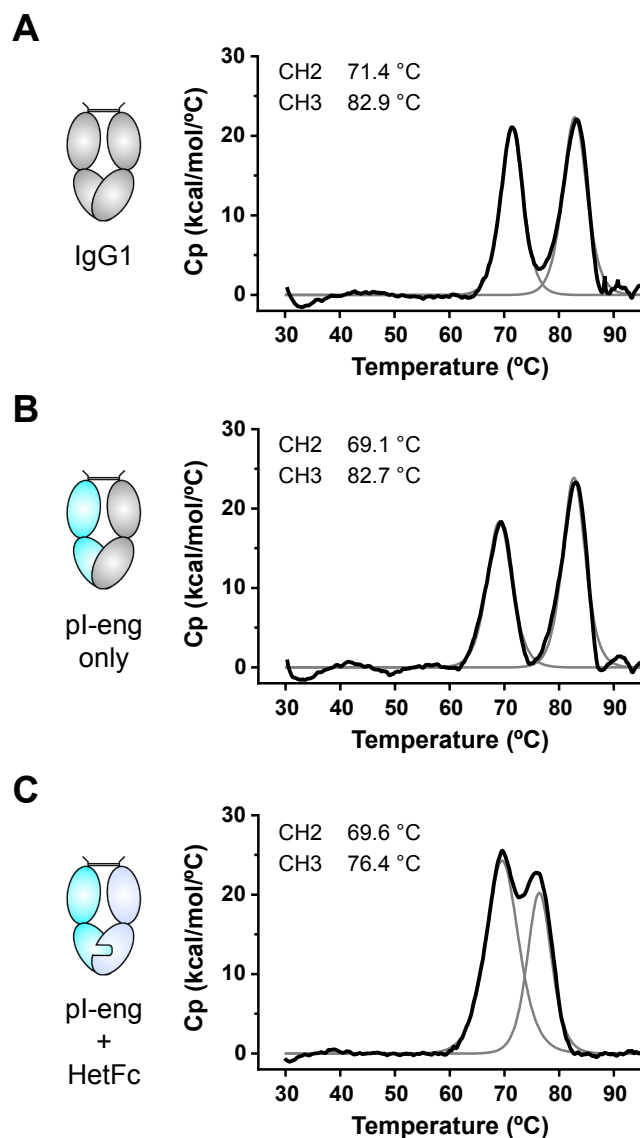


**Fig. 4.** Thermostability of Fc-only system as measured by DSC. (A) Native IgG1, (B) pI engineered (pI-eng) Fc pair, and (C) pI engineered plus heterodimeric Fc (HetFc). Grey lines indicate curve fits describing individual domain melting curves. Melting temperatures and their corresponding domain(s) are listed.

1.5 °C/min. The observed melting profiles were baseline-corrected and normalized using the instrument software. Melting temperatures were determined using the instrument software.

Differential scanning fluorimetry (DSF) thermal denaturation experiments were performed using a CFX Connect Real-Time PCR Detection System (Bio-Rad Laboratories, Inc.). Mixtures of proteins and SYPRO Orange dye were prepared in PBS. Final protein concentration was 0.25 mg/mL; final concentration of the dye was 10X. After initial 10 min incubation at 25 °C, the samples were heated from 25 to 100 °C using a heating rate of 0.5 °C/30 s. A fluorescence reading was taken every 30 s and melting temperatures were determined using the instrument software.

## 2.7. Redirected T cell cytotoxicity (RTCC) assay

Human peripheral blood mononuclear cells (PBMCs) were purified by leukapheresis of anonymous healthy volunteers (HemaCare, Van Nuys, CA) using Ficoll-Paque Plus density gradients (GE Healthcare Life Sciences). Primary human T cells were purified from PBMCs by

**Table 1**

Calculated changes in side chain volume [58] and side chain charge for designed Fc heterodimers and corresponding homodimeric side products.

Variant pairing	Chain 1	Chain 2	$\Delta$ (side chain volume) ( $\text{\AA}^3$ )			$\Delta$ (side chain charge)		
			Chain 1	Chain 2	Net	Chain 1	Chain 2	Net
Heterodimer	S364K	K370S	79.6	-79.6	0.0	1	-1	0
Homodimer	S364K	S364K	79.6	79.6	159.2	1	1	2
Homodimer	K370S	K370S	-79.6	-79.6	-159.2	-1	-1	-2
Heterodimer	E357Q/S364K	L368D/K370S	85.0	-132.2	-47.2	2	-2	0
Homodimer	E357Q/S364K	E357Q/S364K	85.0	85.0	170.0	2	2	4
Homodimer	L368D/K370S	L368D/K370S	-132.2	-132.2	-264.4	-2	-2	-4

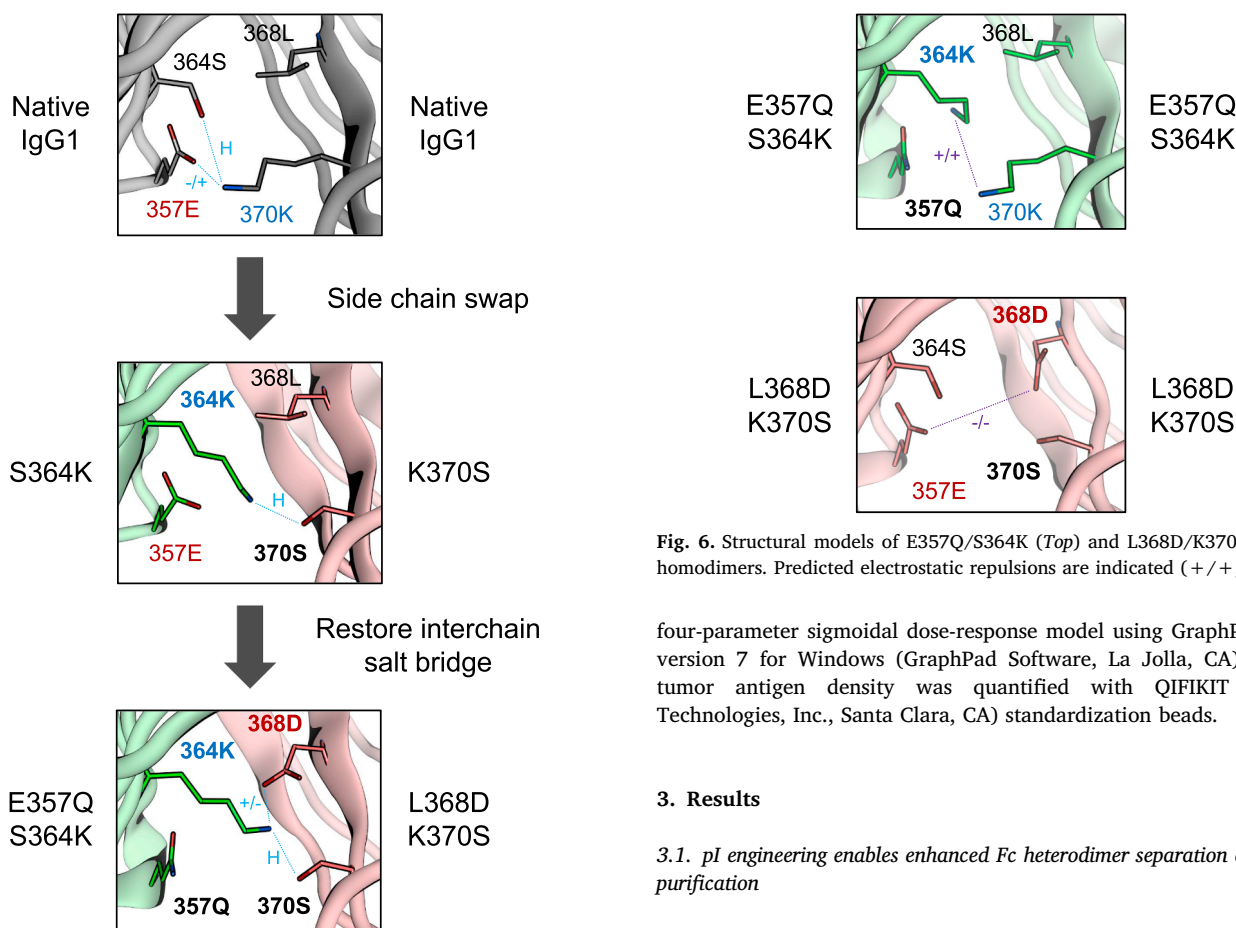


**Fig. 5.** Structural models confirming feasibility of heterodimeric Fc design rationale. Progression from native IgG1 (A) to S364K-K370S heterodimer (B) to E357Q/S364K-L368D/K370S heterodimer (C) is illustrated. Side chains for amino acids at positions 357, 364, 368, and 370 are shown. Protein chain is indicated by ribbon color. Predicted salt bridges (+/-) and hydrogen bonds (H) are labeled. Text color indicates amino acid charge (blue, positive; red, negative), and bold text font indicates amino acid substitution.

negative selection using a T Cell Enrichment Kit (StemCell Technologies, Vancouver, Canada). Tumor target cells were seeded into 96-well plates at 10,000 cells/well. Bispecific antibodies were added in duplicate at the indicated final concentrations. Purified T cells were added at 10:1 effector to target ratio (E:T), and plates were incubated at 37 °C for 24 h. Cells were then incubated with LDH reaction mixture (CytoTox-ONE, Promega, Madison, WI) for 10 min, and fluorescence was measured using a Wallac Victor2 fluorometer (Perkin-Elmer, Waltham, MA). Target cell cytotoxicity (% RTCC) was defined as % RTCC =  $100 \times [(\text{Experimental Value}) - (\text{Target and Effector Mix Background})] / [(\text{Total Target LDH by Detergent Lysis}) - (\text{Spontaneous LDH from Targets})]$ . For  $EC_{50}$  determination, data were fitted with a

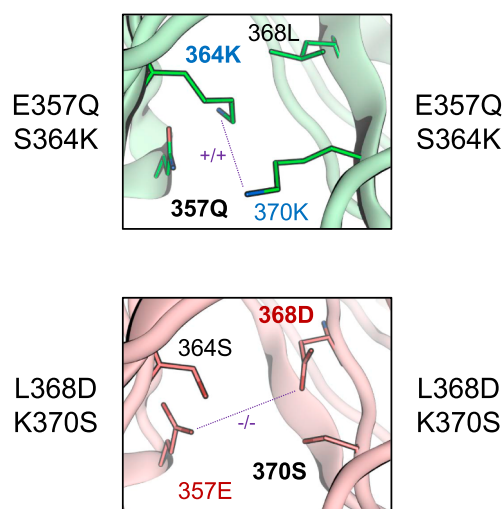


**Fig. 6.** Structural models of E357Q/S364K (Top) and L368D/K370S (Bottom) homodimers. Predicted electrostatic repulsions are indicated (+/+, -/-).

four-parameter sigmoidal dose-response model using GraphPad Prism version 7 for Windows (GraphPad Software, La Jolla, CA). Surface tumor antigen density was quantified with QIFIKIT (Agilent Technologies, Inc., Santa Clara, CA) standardization beads.

### 3. Results

#### 3.1. pI engineering enables enhanced Fc heterodimer separation and purification

We reasoned that engineering a pI differential between the two sides of a heterodimeric Fc by substituting charged residues would result in a heterodimer species having a pI value significantly different than those of potential homodimeric side products. By making changes to the Fc, rather than the Fv, the resulting heterodimeric scaffold could serve as a “one-size-fits-all” purification solution that would allow easy separation of a bispecific heterodimer species using standard IEX purification techniques, independent of the Fv regions and bispecific format. We started by analyzing structural data of a full-length IgG as well as those of the Fc region in complex with Fc $\gamma$  receptors, C1q, FcRn, and protein A (Fig. 2). Using the calculated surface exposure at each position and ensuring that the position did not interact with any of the receptors listed above, we looked for highly exposed D, E, N, and Q residues as targets for substitution to their corresponding isosteric amino acids (i.e., D  $\rightarrow$  N, E  $\rightarrow$  Q, N  $\rightarrow$  D, and Q  $\rightarrow$  E). We reasoned that isosteric amino acid changes have less potential for negatively impacting protein tertiary structure and may be less likely to induce an immunogenic response compared to other pI-altering substitutions. Based on this analysis, several substitutions were identified that should either decrease or increase pI but are predicted to have minimal impact on biophysical properties. Substitutions chosen for incorporation into the

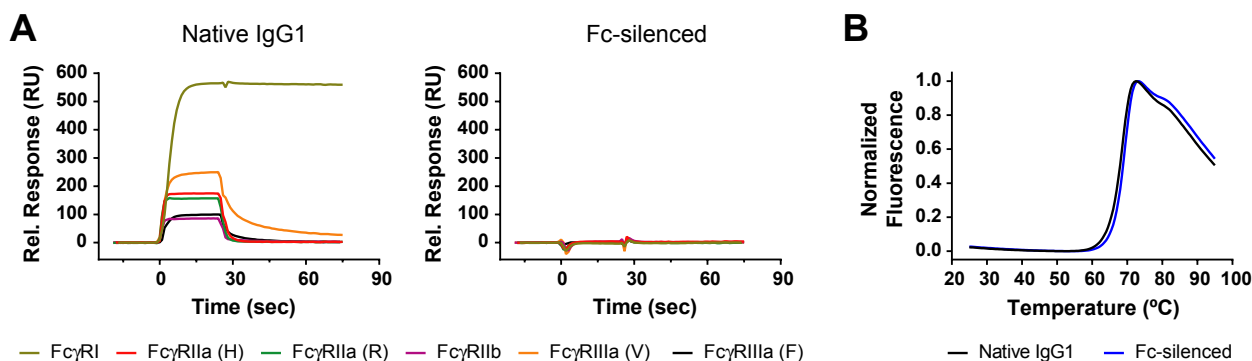


**Fig. 7.** (A) Surface plasmon resonance sensorgrams describing Fc $\gamma$ R binding to native IgG1 and Fc-silenced (E233P/L234V/L235A/G236del/S267K) mAbs. A protein A sensor chip/antibody capture format with receptor as analyte was used, and relative response units after double-referencing are plotted. All Fc $\gamma$ R are at 1  $\mu$ M concentration. Fc $\gamma$ RIIIa alleles 131H and 131R are indicated by H and R. Fc $\gamma$ RIIIa alleles 158V and 158F are indicated by V and F. (B) Thermostability of native IgG1 and Fc-silenced mAbs as measured by DSF.

lower pI Fc heterodimer side were N208D in CH1, Q295E in CH2, and N384D, Q418E, and N421D in CH3. Fc-only protein constructs containing the pI-engineered chain paired with a native IgG1 chain were expressed and analyzed by analytical anion exchange chromatography (AEC) (Fig. 3). Theoretical pI values for the lower pI homodimer, heterodimer, and native IgG1 homodimer were 6.0, 6.4, and 7.3, respectively. As shown in Fig. 3B, the three species are easily separated by a standard IEX method. The resulting distribution of species (lower pI homodimer, heterodimer, and native IgG1) was approximately 25%:50%:25%, indicating that the pI engineering did not introduce any pairing bias. Next, we purified the pI-engineered heterodimeric Fc from its side products by AEC and measured its thermostability by DSC. Two melting transitions were identified at  $T_m$  of 69.1 and 82.7  $^{\circ}$ C, corresponding to the CH2 and CH3 regions, respectively, which are comparable to those measured for native IgG1 ( $T_m$  = 71.4 and 82.9  $^{\circ}$ C, see Fig. 4A and 4B). Although CH2 thermostability was slightly decreased relative to that of native IgG1, it still remained more stable than native IgG2 ( $T_m$  = 68  $^{\circ}$ C) and IgG4 ( $T_m$  = 67  $^{\circ}$ C) [11]. Furthermore, the thermostability of the CH3 region remained constant, critical for it serving as a template for additional Fc engineering for increasing heterodimer yield (see next section).

It should be noted that engineering for a positive shift in pI was much more challenging. We initially identified a set of five potential substitutions to shift to a higher pI consisting of D265N, E269Q, E272Q, E283Q, and E357Q. However, after careful consideration and screening, all but one of these were eliminated from the final design due to either introducing a potential N-linked glycosylation site (D265N), participating in Fc $\gamma$ R binding (E269Q, see Fig. 2), or reducing CH2 thermostability substantially below that of native IgG2 and IgG4 (E272Q and E283Q; data not shown). The remaining substitution, E357Q, is located within the CH3 interface and is utilized in the design of the heterodimeric Fc region, which is described below.

### 3.2. An interfacial side-chain swap enables stable Fc heterodimer design

Our design process began with a study of first-generation Fc heterodimer solutions and the different ways complementarity was introduced at the CH3-CH3 interface: increasing/decreasing side-chain volume (T366W-T366S/L368A/Y407V, knob-into-hole) [8], charge inversions (K409D/K392D-D399K/E356K, electrostatic steering) [9], or multiple IgA substitutions (SEEDbody) [10]. All of these approaches make fairly substantial changes to the interface which could explain the reduced thermostabilities of their CH3 domains ( $T_m$  = 69, 69, and 68  $^{\circ}$ C, respectively). As we were hoping to design a heterodimeric Fc with relatively higher stability, we decided to focus our design efforts around more nuanced changes to the interface while avoiding dramatic changes such as addition/subtraction of aromatic residues and charge

inversions. Along these lines, we adopted a straightforward side-chain swap strategy that would be net isovolumetric. An initial screen of paired isovolumetric and near-isovolumetric substitutions along the CH3-CH3 interface revealed heterodimer yields over 75% (data not shown) for the S364K-K370S pair. In the context of the heterodimer, this side-chain swap is net-isovolumetric (Table 1), minimizing the risk of a destabilizing side-chain packing problem, and should maintain the hydrogen bond between these two positions. Conversely, in the context of the homodimeric side products, the uncompensated volume and charge changes should be unfavorable.

This initial result led us to generate a series of structural models to study this variant and support the development of further design (Figs. 5 and 6). A closer look at the native 364S-370K pair and its neighboring amino acids reveals its participation in two important interchain interactions (Fig. 5A): a hydrogen bond between the hydroxyl group of 364S and the amine group of 370K and a salt bridge between 357E and 370K. While the S364K-K370S variant appears to maintain the hydrogen bond between the two positions, it results in the removal of the native 357E-370K salt bridge (Fig. 5B). Hence, we also explored two additional near-isovolumetric (Table 1) substitutions: (i) L368D, which should re-introduce an interchain salt bridge (S364K-L368D) and (ii) E357Q, which removes the resulting interchain repulsive charge pair (357E-L368D) while also reducing total charge burial. The feasibility of the resulting E357Q/S364K-L368D/K370S combination variant was confirmed by a structural model (Fig. 5C). We also modeled the associated homodimeric side products (Fig. 6). The E357Q/S364K homodimer is predicted to contain a significant electrostatic repulsion and steric clash between S364K and the native 370K, forcing the native 370K to take an altered rotameric state. Likewise, the L368D/K370S homodimer is predicted to contain an electrostatic repulsion, in this case a more distant interaction between the native 357E and L368D, as well as a 10% reduction in buried surface area compared to the native IgG1 interface.

Our newly designed combination variant (E357Q/S364K-L368D/K370S) was constructed and characterized in an Fc-only format. Our test system utilized the pI-engineered Fc pairs discussed above. We made the L368D and K370S substitutions in the background of the lower pI side, as they would potentially synergize with the reduced pI of that chain, while E357Q and S364K were made in the background of native IgG1. Expression in HEK293E cells, protein A purification, and subsequent analysis by analytical-scale anion exchange chromatography revealed a mixture of protein species that was dominated by a high yield (95.1%) of Fc heterodimer (Fig. 3C). Side products consisted of small amounts of E357Q/S364K homodimer (1.7%), E357Q/S364K monomer (1.0%), and L368D/K370S homodimer (2.2%). The expected synergy with the pI engineering was observed (Fig. 3B and C), as the differences in elution times between the heterodimer and the side

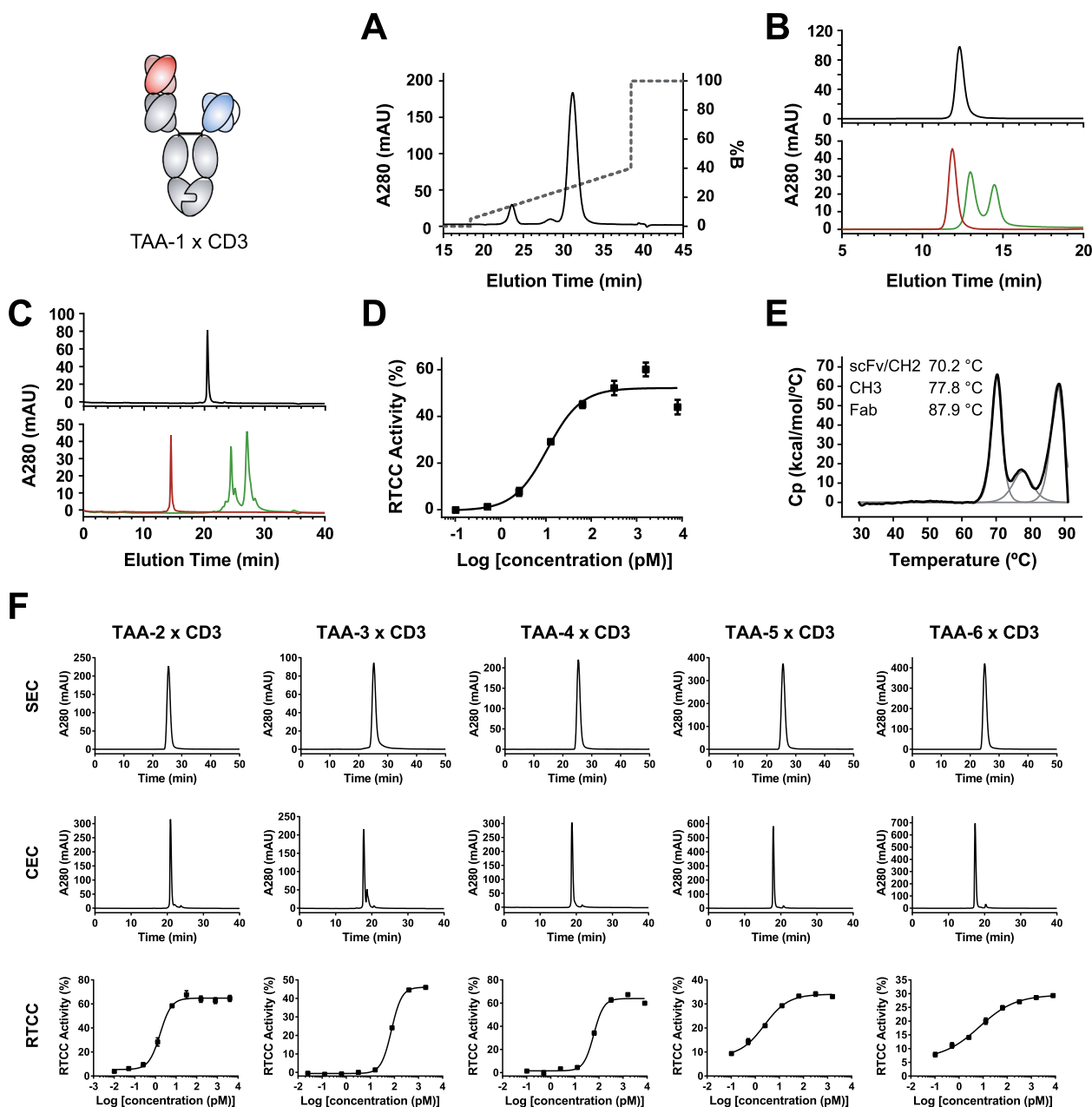


**Fig. 8.** CEC purification and analysis of 1 + 1 Fab-scFv-Fc bispecifics after an initial protein A step. (A) Purification of TAA-1 x CD3 bispecific by CEC. Solid line indicates absorbivity (A280); dotted line indicates elution gradient (%B). (B) *Top*, analysis of the CEC-purified bispecific by analytical SEC. *Bottom*, mAb (red) and scFv-Fc (green) monomers/homodimers overlaid on the same graph for reference. (C) *Top*, analysis of the CEC-purified bispecific by analytical CEC. *Bottom*, mAb (red) and scFv-Fc (green) monomers/homodimers overlaid on the same graph for reference. (D) RTCC activity of the purified bispecific after a 24 h incubation as measured by LDH release (mean  $\pm$  SE of duplicate wells). (E) Thermostability of the CEC-purified bispecific as measured by DSC. Grey lines indicate curve fits describing domain melting curves. Melting temperatures and their corresponding domain(s) are listed. (F) Characterization of five additional TAA x CD3 bispecifics in 1 + 1 format. Shown are analytical SEC (*Top*), analytical CEC (*Middle*), and RTCC activity (*Bottom*) for purified bispecifics. TAA 2–4 target hematological antigens and TAA 5–6 target solid tumor antigens; the same anti-CD3 scFv was used for each bispecific.

products increased slightly.

Next, we purified the E357Q/S364K-L368D/K370S heterodimeric Fc from its side products by anion exchange chromatography and measured its thermostability by DSC (Fig. 4C). Two melting transitions were identified with  $T_m$  of 69.6 (CH2) and 76.4 °C (CH3). The thermostability of the CH3 region was only slightly decreased ( $\Delta T_m = -6.5$  °C) from that measured for the native IgG1 CH3 ( $T_m = 82.9$  °C) and remained more stable than that of the native IgG4 CH3 ( $T_m = 72$  °C). We also expressed and purified the unpaired E357Q/S364K and L368D/K370S proteins and measured their thermostabilities. The CH3 regions of both the E357Q/S364K ( $T_m = 60.5$  °C)

and the L368D/K370S ( $T_m = 67.8$  °C) proteins were highly destabilized relative to both those of the native IgG1 and the E357Q/S364K-L368D/K370S heterodimer, consistent with our expectations from molecular modeling. We also examined the proteins by SEC. Notably, while the L368D/K370S protein was completely dimeric, the E357Q/S364K protein contained 17% monomer (data not shown), accordant with its low thermostability and the 1% monomer observed among the side products. The differences in thermostabilities among the heterodimer and homodimers are in line with the high yield of heterodimer that we observe.

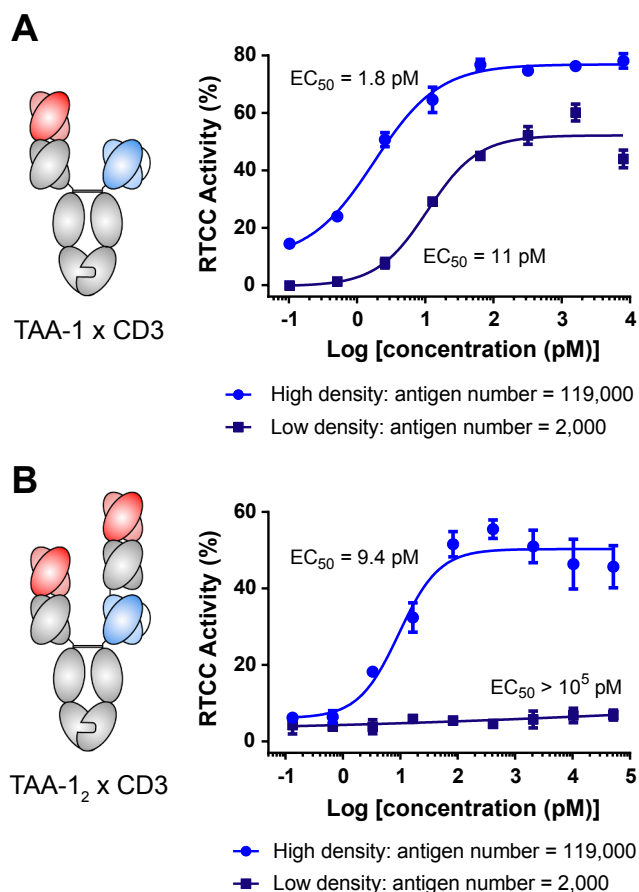


**Fig. 9.** RTCC activity of (A) 1 + 1 and (B) 2 + 1 bispecifics for two cell lines mimicking cancer tissue and normal tissue (high/low antigen density as listed) after a 24 h incubation as measured by LDH release (mean ± SE of duplicate wells). The TAA affinity of the 2 + 1 bispecific is approximately 100-fold weaker than that of the 1 + 1 bispecific. EC<sub>50</sub> values are labeled.

### 3.3. Case study: tumor-associated antigen × CD3 bispecifics

TAA × CD3 bispecifics have been shown to recruit T cells to mediate cytotoxicity against tumor cells, a process known as redirected T cell cytotoxicity (RTCC). One of the most therapeutically advanced examples of a TAA × CD3 bispecific is blinatumomab, a CD19 × CD3 bispecific approved for the treatment of relapsed or refractory acute lymphoblastic leukemia (ALL) [4]. Although blinatumomab is extremely potent, it lacks an Fc domain, and as such its half-life is extremely short ( $t_{1/2} \sim 2$  h), requiring administration by continuous intravenous infusion. Following the success of blinatumomab, next generation TAA × CD3 bispecifics have begun to emerge. The majority of these incorporate an Fc region into their design to increase half-life (e.g., see Refs. [16,19,37–41]).

A critical component of Fc-containing TAA × CD3 bispecifics is the complete ablation of Fc $\gamma$ R binding from the incorporated Fc region, thus eliminating any off-target T cell activation by Fc $\gamma$ R-expressing cells and the potential for T cell lysis mediated by Fc $\gamma$ R-expressing effector cells. Fc $\gamma$ Rs interact with antibodies primarily by contacting the hinge and CH2 domains (see Fig. 2). Human IgG2 antibodies are known to have much weaker affinity for Fc $\gamma$ Rs than human IgG1, and a known driver for this are the differences found in the lower hinge region (positions 230–236) of IgG2. Armour et al. [42] incorporated the lower hinge of IgG2 (E233P/L234V/L235A/G236del) into an IgG1 background and showed that the resulting hybrid Fc lacked Fc $\gamma$ RI binding, analogous to native IgG2. However, also analogous to human IgG2, some affinity for Fc $\gamma$ RII receptors remained. To further silence Fc $\gamma$ R

interaction, we engineered an IgG1 variant that combined the IgG2 lower hinge substitution with an additional CH2 substitution (S267K) at a surface residue previously shown to dramatically modulate Fc $\gamma$ RII affinity [43]. The Fc $\gamma$ R binding of the resulting Fc variant mAb (E233P/L234V/L235A/G236del/S267K) was compared to that of native IgG1 by surface plasmon resonance. As seen in Fig. 7A, binding to Fc $\gamma$  receptors I, IIa, IIb, and IIIa could not be observed. Identical results were seen for mouse and cyno receptors (data not shown). We also established, using differential scanning fluorimetry (DSF), that these Fc $\gamma$ R-silencing substitutions did not affect the thermostability of the CH2 region (Fig. 7B), as the fluorescence transition for both the Fc $\gamma$ R-silencing variant and native IgG1 occurred at near-identical temperatures.

As discussed previously, a robust heterodimeric Fc region enables a wide variety of possible formats (Fig. 1). Initially we focused on a monovalent/monovalent (1 + 1) Fab-scFv-Fc format that permits only monovalent binding to CD3 in the absence of target cells, a critical feature to avoid activation of T cells via CD3 cross-linking. We selected CD3 for the scFv antigen, and stability optimized our scFv to a  $T_m$  of 72 °C to avoid potential developability issues commonly associated with scFvs [44]. To further enable straightforward IEX characterization and purification of the heterodimeric bispecifics, we constructed the anti-CD3 scFv with a pI-increasing (GKPGS)<sub>4</sub> linker between VH and VL and placed it on the high pI (E357Q/S364K) Fc chain, thus further increasing the differences in pI among the heterodimer and its related side products. With this scaffold in place, we incorporated six different anti-TAA variable regions (three targeting hematological antigens and three targeting solid tumor antigens) into the Fab side of the 1 + 1 format. The resulting six TAA × CD3 bispecifics were expressed in HEK293E cells and purified at research-scale by sequential protein A affinity chromatography and CEC. Fig. 8A shows absorbance traces from the CEC purification for the TAA-1 × CD3 bispecific. Purified protein was heterodimeric as shown by SEC-MALS analysis (Fig. 8B), which indicated the expected molecular weight of 127 kDa compared to those of possible side products (53 kDa, monomeric scFv-Fc; 106 kDa, homodimeric scFv-Fc; and 145 kDa, homodimeric Fab-Fc). Higher or lower molecular weight material was undetectable (Fig. 8B) at the limits of the chromatographic system, and although some charge variants were present as expected for an antibody, no signal was detected at an elution time corresponding to homodimeric or monomeric side products of lower or higher pI (see analytical CEC analysis, Fig. 8C). The purified heterodimeric bispecific bound to both targets as expected (data not shown) and was active in an RTCC activity assay with a potency (EC<sub>50</sub>) of 11 pM (Fig. 8D). The thermostability of the TAA-1 × CD3 1 + 1 bispecific was measured by DSC (Fig. 8E). Multiple melting transitions were observed, and we were able to assign each transition to a domain or set of domains. The initial melting transition at a  $T_m$  of 70.2 °C corresponded to the unfolding of the anti-CD3 scFv and the CH2 domains. The next transition at a  $T_m$  of 77.8 °C was assigned to the heterodimeric CH3 domain, corresponding very well to the  $T_m$  of 76.4 °C measured in the Fc-only system above. Finally, the Fab domain underwent a melting transition at a  $T_m$  of 87.9 °C. In general, the 1 + 1 Fab-scFv-Fc format exhibited thermostability in the range expected of well-behaved therapeutic antibodies. Further TAA × CD3 bispecifics were produced and assessed in a similar manner, and all showed near 100% homogeneity, and RTCC potencies ranging from 2 to 75 pM (Fig. 8F). These data demonstrate that the combination of our engineered Fc with the 1 + 1 Fab-scFv-Fc format are accepting of a broad range of Fab regions and validates this combination for producing well-behaved and active T-cell directed CD3 bispecifics.

To develop optimal TAA × CD3 bispecifics, a more systematic assessment of the TAA biology in the potential patient population(s) has become integral to the design process. Factors such as tumor load, cell surface antigen density, and normal tissue expression all impact the pharmacodynamics and tolerability. To date, these complexities have been addressed empirically [37,45,46]. Reducing the affinity of the

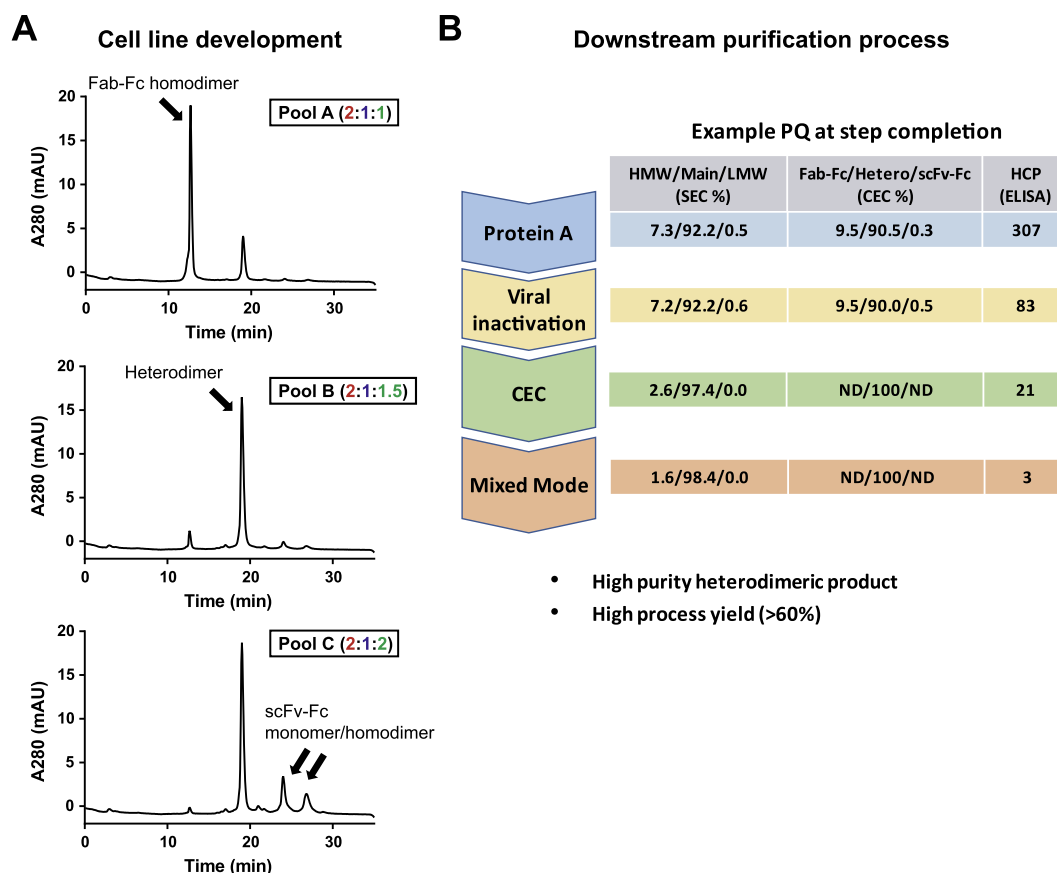


**Fig. 10.** Manufacturing of heterodimeric Fc bispecifics. (A) Optimization of DNA ratios during transfection to generate stable pools with preferential production of heterodimeric bispecific. In this example of a 1 + 1 molecule, monocistronic plasmid vectors encoding light chain (red), Fab-Fc (blue) and scFv-Fc (green) were mixed in various ratios and transfected in CHO-M cells using electroporation. After selection and expansion, stable pools generated were grown in shake flask fed-batch cultures. Harvested supernatants were purified using protein A chromatography and analyzed by analytical CEC to assess heterodimer yield. Changes in scFv-Fc DNA amounts have the most impact on optimum heterodimer production. The best stable pool was subjected to two rounds of single cell cloning and analyses to obtain the ideal production cell line typically producing > 90% heterodimer. (B) Summary of downstream purification process utilized to produce high purity heterodimeric bulk drug substance. The three-step high-yield process uses standard resins routinely employed in commercial manufacture of monoclonal antibodies. The pI differences between homodimers and the heterodimer enable their effective separation during the CEC step, while the final polishing step using mixed mode resin effectively removes all product and host related impurities.

CD3 binder has been shown to improve pharmacokinetics and attenuate cytokine release [45,46]. Furthermore, a 2 + 1 format, bivalent for TAA and monovalent for CD3, with relatively weak TAA affinity, has been shown to exhibit preferential cytotoxicity of high-expressing tumor cells over low-expressing normal cells [37]. Thus, as an extension to our 1 + 1 Fab-scFv-Fc platform, we designed the 2 + 1 Fab<sub>2</sub>-scFv-Fc format (Fig. 1) to allow for TAA bivalency while retaining CD3 monovalency.

In a specific case study for the TAA-1 presented above, we wished to explore the impact on pharmacology and selectivity of different valencies for the TAA and different affinities for both TAA and CD3. Our goal was to engineer a tuned bispecific with RTCC activity on high TAA-1 expressing tumor tissue and little or no RTCC activity on low expressing normal tissue. Semi-quantitative IHC (data not shown) was performed on a set of tumor and normal tissues and a set of cell lines to identify a high-density cell line to mimic cancer tissue (approximately 119,000 TAA per cell) and a low-density cell line to mimic normal tissue (approximately 2000 TAA per cell). We also engineered a panel of TAA-1 Fabs and CD3 scFvs with varied affinities. A panel of 2 + 1 bispecifics was produced using the same methods as described above for 1 + 1 bispecifics, and the 2 + 1 format demonstrated comparable behavior and thermostability (data not shown). We then examined the activity of the 2 + 1 bispecifics in an RTCC assay, and present the results for a highly selective 2 + 1 bispecific with weakened TAA-1 (approximately 100-fold weaker, data not shown) and CD3 affinities. The

1 + 1 bispecific presented earlier (Fig. 8A–E) mediated highly potent cytotoxicity of both high and low TAA-1 expressing cells (Fig. 9A), while, strikingly, the 2 + 1 bispecific mediated cytotoxicity of only high TAA-1 expressing cells while completely sparing low TAA-1 expressing cells (Fig. 9B). The selectivity exhibited by the 2 + 1 format is similar to what has been described elsewhere [37], and potentially empowers TAA × CD3 bispecifics to address an expanded set of tumor antigen biologics.

### 3.4. Translation to manufacturing scale

During the engineering and design phases of our heterodimeric Fc platform careful attention was paid to enable correct assembly of the heterodimeric bispecific as well as minimize the amounts of undesired side products. For making a successful therapeutic entity using this platform, this had to be translated at manufacturing scale using established methods of expression and purification that are easy to implement and transfer as needed. The manufacturing process started with first developing a stable cell line expressing primarily the properly assembled heterodimer. Our first experience was with a 1 + 1 Fab-scFv-Fc molecule targeting a TAA and CD3. We transfected CHO-M cells with optimized ratios of vectors encoding each of the three chains (light chain, Fab-Fc, and scFv-Fc) to generate multiple stable pools. Product quality and titer were evaluated for each of these pools after fed-batch culture, and protein A purified material was analyzed by SEC and CEC

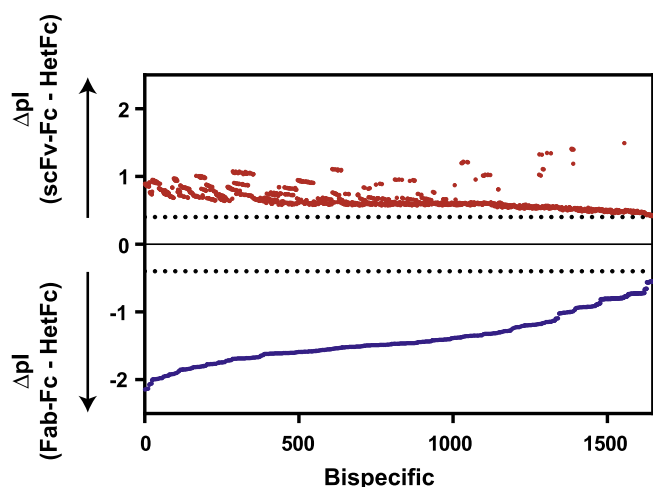


**Fig. 11.** In silico analysis of pI differences between bispecific heterodimer and homodimer side products for all possible bispecific combinations created using 58 approved antibody Fv sequences. 1653 bispecifics and their corresponding homodimer sequences were constructed and theoretical pIs calculated. To create bispecific sequences, Fvs were inserted into both the Fab and scFv of the 1 + 1 Fab-scFv-Fc format containing our pI, heterodimer, and Fc-silencing substitutions along with a charged (GKPGS)<sub>4</sub> linker in the scFv. Dashed lines indicate a  $\Delta$ pI of 0.4 units, which is a difference that results in straightforward separation of the bispecific in our case study. Using this cutoff, our Fc heterodimer technology coupled with the 1 + 1 Fab-scFv-Fc format would allow IEX separation of the bispecific species 100% of the time and is thus compatible with all currently approved antibody Fvs.

to determine the heterodimer/homodimer distribution (Fig. 10A). Stable pools with the best heterodimer production (typically > 85% at this stage) were subjected to two rounds of clonal isolation to generate monoclonal cell lines that were ranked by their titers and product quality after fed-batch and bioreactor cultivations. We have successfully generated stable cell lines using this platform for more than 10 Fab-scFv-Fc molecules (1 + 1) with titers ranging from 2.5 to 5.0 g/L in controlled bioreactors (50 L to 2000 L), with greater than 90% desired heterodimer bispecific product being produced in harvest.

Commercial purification processes for monoclonal antibodies

**Table 2**

Comparison of the current work and published Fc heterodimer solutions showing reported heterodimer yields and thermostabilities listed in approximately chronological order.

Chain 1	Chain 2	Hetero-Fc yield	C <sub>H3</sub> T <sub>m</sub> (°C)	IgG1 C <sub>H3</sub> T <sub>m</sub> (°C)	C <sub>H3</sub> $\Delta$ T <sub>m</sub> (°C)	Ref.
T366W	T366S/L368A/Y407V	95%	69.4	80.4	-11	[6]
T366W/S354C	T366S/L368A/Y407V/Y349C	95%	n.r. <sup>†</sup>	n.r. <sup>†</sup>	n.r. <sup>†</sup>	[7]
Multiple IgA subs.	Multiple IgA subs.	85–95%	67.9	82.5	-14.6	[10,59]
K409D/K392D	D399K/E356K	100%	68.8	82.9	-14.1	[9]
S364H/F405A	Y349T/T394F	89%	69	83	-14	[12]
D221E/P228E/L368E	D221R/P228R/K409R	90–100%	71–80	82	-11	[19]
F405L	K409R	94.6% <sup>‡</sup>	72.6	n.r.	-10.4 <sup>‡</sup>	[60]
T350V/T366L/K392L/T394W	T350V/L351Y/F405A/Y407V	> 95%	81.5	82.4	-0.9	[61]
Multiple TCR $\alpha$ subs.	Multiple TCR $\beta$ subs.	96%	69.5	n.r.	-13.5 <sup>‡</sup>	[15]
K360E/K409W	Q347R/D399V/F405T	91%	77.5	86	-8.5	[62]
K360E/K409W/Y349C	Q347R/D399V/F405T/S354C	94%	80.2	85.4	-5.2	[63]
K370E/K409W	E357N/D399V/F405T	93.4%	76.9	85.3	-8.4	[64]
K360D/D399M/Y407A	E345R/Q347R/T366V/K409V	93.3%	70.4	82.9	-12.5	[65]
Y349S/K370Y/T366M/K409V	E356G/E357D/S364Q/Y407A	94.2%	68.9	82.9	-14	[65]
L351D/L368E	L351K/T366K	~99%	69.5	82.5	-13	[49]
L368D/K370S <sup>§</sup>	E357Q/S364K <sup>§</sup>	95.1%	76.4	82.9	-6.5	-

<sup>†</sup> n.r.: not reported.

<sup>\*</sup> After separate expression/purification of homodimers followed by controlled Fab-arm exchange.

<sup>\*</sup> Calculated using a native IgG1 CH3 T<sub>m</sub> = 83 °C.

<sup>§</sup> Data is reported in the context of pI-engineered Fc pairs.

typically use 3 steps – protein A followed by ion-exchange and polish steps to remove product-related (e.g., aggregates) and host-related (DNA, HCP, etc.) impurities. Our heterodimeric Fc platform was designed with this in mind, and we were able to use standard resins to create a process that effectively removes all the undesired species and impurities and still maintains high process yields (> 60%) typical of commercial monoclonal antibody purification. The bispecific heterodimer is also very stable at low pH, enabling a standard viral inactivation step to be used. After the initial protein A step, the product contains greater than 90% heterodimer with minimal aggregate. Analogous to the research-scale process, the homodimeric side products are removed to below detection levels using a CEC step. This and the subsequent polish step using a mixed mode resin effectively removes all the product and host related impurities. This platform process has been used to complete more than 6 GMP campaigns for different 1 + 1 molecules to date, confirming the robustness of the process (Fig. 10B). Ongoing stability assessments on the final liquid formulations for multiple TAA  $\times$  CD3 molecules indicate that they are very stable, with no impact on aggregation, heterodimer/homodimer ratios and bioactivity over long periods of refrigerated and frozen storage (data generated at testing CROs and included in regulatory filings).

#### 4. Discussion

Heterodimeric Fc technology has been utilized to produce many different formats of bispecific antibodies, with one of these bispecifics an already approved therapeutic [3] and many more that are currently in clinical trials. Herein we have demonstrated engineering of an improved heterodimeric Fc technology, called the XmAb bispecific platform, that retains the efficient development properties of a mAb. As potential immunogenicity is a concern with all engineered protein therapeutics, we sought to minimize the risk of immunogenicity by utilizing buried and isosteric amino acid substitutions that should result in minimal perturbation of protein tertiary structure, although the final assessment of immunogenicity will have to be determined from clinical data. We demonstrated the utility of our technology in the context of T cell recruiting TAA  $\times$  CD3 bispecifics, and demonstrated expansion of this platform to enable a 2 + 1 TAA<sub>2</sub>  $\times$  CD3 format.

Although our technology results in very small amounts of homodimer impurities being produced, we have demonstrated that these can

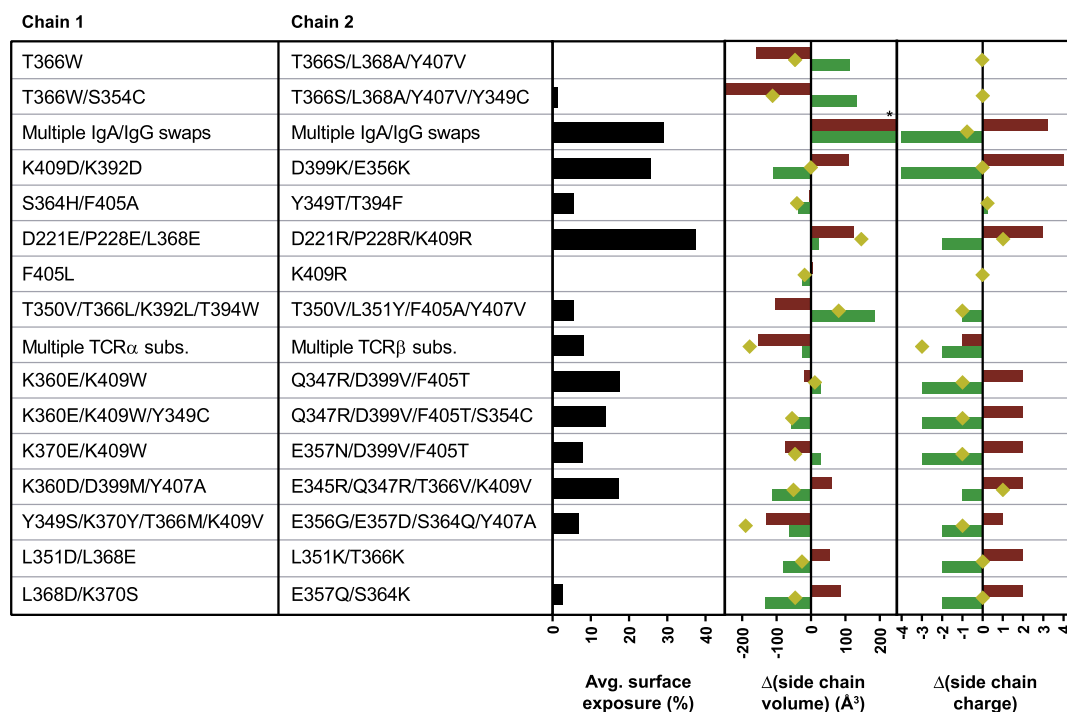


**Fig. 12.** Meta-analysis of the current work and published heterodimeric Fc solutions (listed in approximately chronological order; references listed in Table 2). Average surface exposure was calculated as described for Fig. 2. Changes in side chain volume and charge are calculated as in Table 1. Red bars: Chain 1; green bars: Chain 2; gold diamonds: net change. \* indicates  $\Delta$  (side chain volume)  $> 225 \text{ \AA}^3$ .

be efficiently removed with industry-standard purification methods due to our incorporated pI engineering component. Other groups have taken several different approaches to purifying the desired bispecific heterodimer species from homodimer side products. One such method utilized by several groups [14–17] takes advantage of the isotopic substitution H435R present in IgG3 which abolishes binding of the Fc to protein A. By using an asymmetric Fc with H435R on one-side, selective pH elution of the desired heterodimer bispecific can be achieved, as the homodimer H435R-H435R will not bind protein A and the native 435H-435H will bind more strongly than the heterodimer 435H-H435R. This method can be complicated by the fact that some variable regions, particularly those with VH class 3 frameworks, also bind protein A [47]. Moreover, the 435H residue participates in FcRn binding, and it has been shown that IgG1-H435R has faster in vivo clearance [48]. However, it is unknown if this substitution on only one side of the Fc compromises half-life, and Smith et al. [16] report a quite acceptable half-life of 14 days for a CD20  $\times$  CD3 bispecific containing a single H435R substitution. Other groups, as well as the approach taken herein, utilize charge/pI differences in the heterodimer and homodimer species to enable IEX separation [18,19,49]. Sharkey et al. [18] claim the ability to produce native IgG1-like bispecific mAbs with a common-light chain approach and by purification with “highly linear pH gradients” to separate desired bispecific species with isoelectric points that can differ in as little as 0.1 units from side products. However, this method requires complicated mixtures of many different biological buffers and it is unclear if the approach will be viable at manufacturing scale. Our method utilizes industry-standard IEX purification and will result in favorable separation profiles with nearly any possible combination of Fv regions. In our case study 1 + 1 Fab-scFv-Fc TAA-1  $\times$  CD3 example, the calculated pI values of the three species were 7.9 (homodimer), 8.7 (heterodimer), and 9.1 (homodimer) – a difference of only 0.4 pI units between the heterodimer and high-pI homodimer, and we were able to completely separate the heterodimer species (Fig. 8A–C). As an in silico analysis, we constructed (in the 1 + 1 Fab-scFv-Fc format containing pI, heterodimer, and Fc-silencing substitutions and using our charged linker in the scFv) all possible bispecifics with Fv

pairs from 58 currently approved antibodies listed in the Tabs database [5]. Assuming a requirement of a  $\Delta$ pI of 0.4 units between any heterodimer and its homodimer species, this exercise demonstrates that we would theoretically achieve separation of side-products in 100% of cases (Fig. 11).

We benchmarked our lead heterodimeric Fc variant versus other published solutions. As seen in Table 2, many solutions exist for achieving relative heterodimer yields of over 90%, with varying degrees of CH3 region destabilization. Our E357Q/S364K-L368D/K370S variant results in a CH3 region that remained more stable than that of native IgG4. We performed a further analysis of the multitude of design strategies that have been used (Fig. 12). While substitutions have been made at almost every position along the CH3-CH3 interface, our analysis is still able to reveal some general trends. The majority of published solutions utilize positions that are completely buried, such as 366 and 409. Our variant is no exception, as positions 357, 364, and 368 are completely buried, while position 370 is only partially exposed. Only a few solutions substitute at exposed positions, and involve either the inversion (K409D/K392D-D399K/E356K) or insertion (D221E/P228E/L368E-D221R/P228R/K409R, K360E/K409W-Q347R/D399V/F405T, K370E/K409W-E357N/D399V/F405T) of electrostatic interactions at the periphery of the interface. We also see a trend away from the initial “knob-into-hole” solution (T366W-T366S/L368A/Y407V), which relied on large, opposing changes in side chain volume to promote heterodimerization, toward solutions involving electrostatic interactions (Fig. 12). Our own solution could be called a hybrid of these two approaches in that we introduce a modest change in both volume and charge. Incorporation of an electrostatic component into our design provided synergy with the pI-engineered Fc regions presented above, allowing industry-standard IEX purification of the heterodimeric species.

In our case study describing application of our Fc heterodimer technology, we focus on TAA  $\times$  CD3 bispecifics, an important and promising new class of therapeutics. For these examples we use a 1 + 1 Fab-scFv-Fc format for monovalent TAA  $\times$  CD3 targeting as well as a 2 + 1 Fab<sub>2</sub>-scFv-Fc format for bivalent TAA<sub>2</sub>  $\times$  CD3 targeting.

Although not the main focus of this paper, it deserves mention that both of these formats can be produced in good yields and high purity (Fig. 8A–C), are biophysically well-behaved as demonstrated from our DSC data (Fig. 8E), and, although not highlighted herein, exhibit antibody-like pharmacokinetics. Although it may be argued that a 1 + 1 common light chain format may be more desirable due to its native IgG architecture and lack of scFvs, we find that the Fab-scFv-Fc format makes a useful platform in cases, like CD3 bispecifics, where the same Fv can be paired with many different “off-the-shelf” Fab regions to quickly generate therapeutic bispecific candidates (Fig. 8F). Our 2 + 1 TAA<sub>2</sub> × CD3 format, as demonstrated in our case study, has proven to be extremely useful in avoiding cytotoxicity of low TAA expressing normal tissue while still achieving high potency killing of high TAA expressing cancer cell lines. As shown in Fig. 9, having both of these bispecific formats on hand, enabled by our heterodimeric Fc, allows us to tune activity on a case-by-case basis depending on the TAA biology. Another important component of our case study is the incorporation of the IgG2 lower hinge + S267K substitution to abolish FcγR and C1q binding. These substitutions maintained native IgG1 stability and effectively abolished FcγR and C1q binding more effectively than any natural isotype.

Although not discussed in this manuscript, we have since utilized our heterodimeric Fc to produce several other TAA × CD3 bispecifics (CD123 × CD3 in the clinic as XmAb14045 [50]; CD20 × CD3 in the clinic as XmAb13676 [51]; SSTR2 × CD3 in the clinic as XmAb18087 [52]; and CD38 × CD3 in the clinic as AMG 424 [46,53]), dual-checkpoint blockade bispecifics (PD-1 × CTLA-4 in the clinic as XmAb20717 [54], and CTLA-4 × LAG-3 soon to be in the clinic as XmAb22841 [55]), and a checkpoint × costimulatory receptor bispecific (PD-1 × ICOS soon to be in the clinic as XmAb23104 [56]). Newer formats produced include various cytokine and mAb-cytokine fusions utilizing IL-15 [57], some of which are shown in Fig. 1. In all cases, biophysical properties and overall heterodimer yield have been comparable to that described in our case study. Our Fc heterodimer technology has proven to be an efficient component to rapidly enable multiple clinical bispecific candidates.

## Acknowledgements

We thank Kendra Avery and Dave Lu for assisting with the DSC experiments, and Greg LaBelle for coordinating the manufacturing activities. We would also like to thank the cell line development team at Selexis, and both upstream and downstream process development and manufacturing teams at KBI for their valuable insights, helpful discussions and efficient translation to a commercial process.

## References

- [1] P.J. Carter, G.A. Lazar, Next generation antibody drugs: pursuit of the ‘high-hanging fruit’, *Nat. Rev. Drug Discov.* 17 (3) (2018) 197–223.
- [2] U. Brinkmann, R.E. Kontermann, The making of bispecific antibodies, *MAbs* 9 (2) (2017) 182–212.
- [3] T. Kitazawa, T. Igawa, Z. Sampei, A. Muto, T. Kojima, T. Soeda, K. Yoshihashi, Y. Okuyama-Nishida, H. Saito, H. Tsunoda, T. Suzuki, H. Adachi, T. Miyazaki, S. Ishii, M. Kamata-Sakurai, T. Iida, A. Harada, K. Esaki, M. Funaki, C. Moriyama, E. Tanaka, Y. Kikuchi, T. Wakabayashi, M. Wada, M. Goto, T. Toyoda, A. Ueyama, S. Suzuki, K. Haraya, T. Tachibana, Y. Kawabe, M. Shima, A. Yoshioka, K. Hattori, A bispecific antibody to factors Ixα and X restores factor VIII hemostatic activity in a hemophilia A model, *Nat. Med.* 18 (10) (2012) 1570–1574.
- [4] R. Bargou, E. Leo, G. Zugmaier, M. Klingler, M. Goebeler, S. Knop, R. Noppeney, A. Viardot, G. Hess, M. Schuler, H. Einsele, C. Brandl, A. Wolf, P. Kirchinger, P. Klappers, M. Schmidt, G. Riethmuller, C. Reinhardt, P.A. Baeuerle, P. Kufner, Tumor regression in cancer patients by very low doses of a T cell-engaging antibody, *Science* 321 (5891) (2008) 974–977.
- [5] <http://tabs.craic.com/>. (Accessed 7/20/2018).
- [6] S. Atwell, J.B. Ridgway, J.A. Wells, P. Carter, Stable heterodimers from remodeling the domain interface of a homodimer using a phage display library, *J. Mol. Biol.* 270 (1) (1997) 26–35.
- [7] A.M. Merchant, Z. Zhu, J.Q. Yuan, A. Goddard, C.W. Adams, L.G. Presta, P. Carter, An efficient route to human bispecific IgG, *Nat. Biotechnol.* 16 (7) (1998) 677–681.
- [8] J.B. Ridgway, L.G. Presta, P. Carter, ‘Knobs-into-holes’ engineering of antibody CH3 domains for heavy chain heterodimerization, *Protein Eng.* 9 (7) (1996) 617–621.
- [9] K. Gunasekaran, M. Pentony, M. Shen, L. Garrett, C. Forte, A. Woodward, S.B. Ng, T. Born, M. Retter, K. Manchulenko, H. Sweet, I.N. Foltz, M. Wittekind, W. Yan, Enhancing antibody Fc heterodimer formation through electrostatic steering effects: applications to bispecific molecules and monovalent IgG, *J. Biol. Chem.* 285 (25) (2010) 19637–19646.
- [10] J.H. Davis, C. Aperlo, Y. Li, E. Kurosawa, Y. Lan, K.M. Lo, J.S. Huston, SEEDbodies: fusion proteins based on strand-exchange engineered domain (SEED) CH3 heterodimers in an Fc analogue platform for asymmetric binders or immunofusions and bispecific antibodies, *Protein Eng. Des. Sel.* 23 (4) (2010) 195–202.
- [11] E. Garber, S.J. Demarest, A broad range of Fab stabilities within a host of therapeutic IgGs, *Biochem. Biophys. Res. Commun.* 355 (3) (2007) 751–757.
- [12] G.L. Moore, C. Bautista, E. Pong, D.H. Nguyen, J. Jacinto, A. Eivazi, U.S. Muchhal, S. Karki, S.Y. Chu, G.A. Lazar, A novel bispecific antibody format enables simultaneous bivalent and monovalent co-engagement of distinct target antigens, *MAbs* 3 (6) (2011) 546–557.
- [13] J.H. Ha, J.E. Kim, Y.S. Kim, Immunoglobulin Fc heterodimer platform technology: from design to applications in therapeutic antibodies and proteins, *Front. Immunol.* 7 (2016) 394.
- [14] Y. Mazor, V. Oganessian, C. Yang, A. Hansen, J. Wang, H. Liu, K. Sachsenmeier, M. Carlson, D.V. Gadre, M.J. Borrok, X.Q. Yu, W. Dall’Acqua, H. Wu, P.S. Chowdhury, Improving target cell specificity using a novel monovalent bispecific IgG design, *MAbs* 7 (2) (2015) 377–389.
- [15] D. Skegco, C. Stutz, R. Ollier, E. Svensson, P. Wassmann, F. Bourquin, T. Monney, S. Gn, S. Blein, Immunoglobulin domain interface exchange as a platform technology for the generation of Fc heterodimers and bispecific antibodies, *J. Biol. Chem.* 292 (23) (2017) 9745–9759.
- [16] E.J. Smith, K. Olson, L.J. Haber, B. Varghese, P. Duramad, A.D. Tustian, A. Oyejide, J.R. Kirshner, L. Canova, J. Menon, J. Principio, D. MacDonald, J. Kantrowitz, N. Papadopoulos, N. Stahl, G.D. Yancopoulos, G. Thurston, S. Davis, A novel, native-format bispecific antibody triggering T-cell killing of B-cells is robustly active in mouse tumor models and cynomolgus monkeys, *Sci. Rep.* 5 (2015) 17943.
- [17] A.D. Tustian, C. Endicott, B. Adams, J. Mattila, H. Bak, Development of purification processes for fully human bispecific antibodies based upon modification of protein A binding avidity, *MAbs* 8 (4) (2016) 828–838.
- [18] B. Sharkey, S. Pudi, I. Wallace Moyer, L. Zhong, B. Prinz, H. Baruah, H. Lynaugh, S. Kumar, K.D. Wittrup, J.H. Nett, Purification of common light chain IgG-like bispecific antibodies using highly linear pH gradients, *MAbs* 9 (2) (2017) 257–268.
- [19] P. Strop, W.H. Ho, L.M. Boustany, Y.N. Abdiche, K.C. Lindquist, S.E. Farias, M. Rickert, C.T. Appah, E. Pascua, T. Radcliffe, J. Sutton, J. Chaparro-Riggers, W. Chen, M.G. Casas, S.M. Chin, O.K. Wong, S.H. Liu, G. Vergara, D. Shelton, A. Rajpal, J. Pons, Generating bispecific human IgG1 and IgG2 antibodies from any antibody pair, *J. Mol. Biol.* 420 (3) (2012) 204–219.
- [20] Z. Sampei, T. Igawa, T. Soeda, Y. Okuyama-Nishida, C. Moriyama, T. Wakabayashi, E. Tanaka, A. Muto, T. Kojima, T. Kitazawa, K. Yoshihashi, A. Harada, M. Funaki, K. Haraya, T. Tachibana, S. Suzuki, K. Esaki, Y. Nabuchi, K. Hattori, Identification and multidimensional optimization of an asymmetric bispecific IgG antibody mimicking the function of factor VIII cofactor activity, *PLoS One* 8 (2) (2013) e57479.
- [21] Y. Durocher, S. Perret, A. Kamen, High-level and high-throughput recombinant protein production by transient transfection of suspension-growing human 293-EBNA1 cells, *Nucl. Acids Res.* 30 (2) (2002) E9.
- [22] E.A. Kabat, T.T. Wu, H.M. Perry, K.S. Gottesman, C. Foeller, Sequences of Proteins of Immunological Interest, fifth ed., U.S. Department of Health and Human Services, Bethesda, MD, 1991.
- [23] E.O. Saphire, P.W. Parren, R. Pantophlet, M.B. Zwick, G.M. Morris, P.M. Rudd, R.A. Dwek, R.L. Stanfield, D.R. Burton, I.A. Wilson, Crystal structure of a neutralizing human IGG against HIV-1: a template for vaccine design, *Science* 293 (5532) (2001) 1155–1159.
- [24] M. Kiyoshi, J.M. Caaveiro, T. Kawai, S. Tashiro, T. Ide, Y. Asaoka, K. Hatayama, K. Tsumoto, Structural basis for binding of human IgG1 to its high-affinity human receptor FcγRI, *Nat. Commun.* 6 (2015) 6866.
- [25] P.A. Ramsland, W. Farrugia, T.M. Bradford, C.T. Sardjono, S. Esparon, H.M. Trist, M.S. Powell, P.S. Tan, A.C. Cendron, B.D. Wines, A.M. Scott, P.M. Hogarth, Structural basis for Fc γRIIIa recognition of human IgG and formation of inflammatory signaling complexes, *J. Immunol.* 187 (6) (2011) 3208–3217.
- [26] F. Mimoto, H. Katada, S. Kadono, T. Igawa, T. Kuramochi, M. Muraoka, Y. Wada, K. Haraya, T. Miyazaki, K. Hattori, Engineered antibody Fc variant with selectively enhanced FcγRIIb binding over both FcγRIIIa(R131) and FcγRIIIa(H131), *Protein Eng. Des. Sel.* 26 (10) (2013) 589–598.
- [27] C. Ferrara, S. Grau, C. Jager, P. Sonderrmann, P. Brunker, I. Waldhauer, M. Hennig, A. Ruf, A.C. Rufer, M. Stihle, P. Umama, J. Benz, Unique carbohydrate-carbohydrate interactions are required for high affinity binding between FcγRIII and antibodies lacking core fucose, *Proc. Natl. Acad. Sci. U. S. A.* 108 (31) (2011) 12669–12674.
- [28] S. Radaev, S. Motyka, W.H. Fridman, C. Sautes-Fridman, P.D. Sun, The structure of a human type III FcγRIII receptor in complex with Fc, *J. Biol. Chem.* 276 (19) (2001) 16469–16477.
- [29] V. Oganessian, M.M. Damschroder, K.E. Cook, Q. Li, C. Gao, H. Wu, W.F. Dall’Acqua, Structural insights into neonatal Fc receptor-based recycling mechanisms, *J. Biol. Chem.* 289 (11) (2014) 7812–7824.
- [30] J. Deisenhofer, Crystallographic refinement and atomic models of a human Fc fragment and its complex with fragment B of protein A from *Staphylococcus aureus* at 2.9- and 2.8-Å resolution, *Biochemistry* 20 (9) (1981) 2361–2370.
- [31] Molecular Operating Environment (MOE), Chemical Computing Group ULC, Montreal, QC, Canada, H3A 2R7, 2018.
- [32] D. Ugurlar, S.C. Howes, B.J. de Kreuk, R.I. Koning, R.N. de Jong, F.J. Beurskens,

- J. Schuurman, A.J. Koster, T.H. Sharp, P. Parren, P. Gros, Structures of C1-IgG1 provide insights into how danger pattern recognition activates complement, *Science* 359 (6377) (2018) 794–797.
- [33] S. Matsumiya, Y. Yamaguchi, J. Saito, M. Nagano, H. Sasakawa, S. Otaki, M. Satoh, K. Shitara, K. Kato, Structural comparison of fucosylated and nonfucosylated Fc fragments of human immunoglobulin G1, *J. Mol. Biol.* 368 (3) (2007) 767–779.
- [34] A. Sillero, A. Maldonado, Isoelectric point determination of proteins and other macromolecules: oscillating method, *Comput. Biol. Med.* 36 (2) (2006) 157–166.
- [35] B. Bjellqvist, B. Basse, E. Olsen, J.E. Celis, Reference points for comparisons of two-dimensional maps of proteins from different human cell types defined in a pH scale where isoelectric points correlate with polypeptide compositions, *Electrophoresis* 15 (3–4) (1994) 529–539.
- [36] J.O. Richards, S. Karki, G.A. Lazar, H. Chen, W. Dang, J.R. Desjarlais, Optimization of antibody binding to Fcγ<sub>2</sub> enhances macrophage phagocytosis of tumor cells, *Mol. Cancer Ther.* 7 (8) (2008) 2517–2527.
- [37] M. Bacac, T. Fauti, J. Sam, S. Colombetti, T. Weinzierl, D. Ouaret, W. Bodmer, S. Lehmann, T. Hofer, R.J. Hosse, E. Moessner, O. Ast, P. Bruenker, S. Grau-Richards, T. Schaller, A. Seidl, C. Gerdes, M. Perro, V. Nicolini, N. Steinhoff, S. Dudal, S. Neumann, T. von Hirschheydt, C. Jaeger, J. Saro, V. Karanikas, C. Klein, P. Umama, A novel carcinoembryonic antigen T-Cell bispecific antibody (CEA TCB) for the treatment of solid tumors, *Clin. Cancer Res.* 22 (13) (2016) 3286–3297.
- [38] G. Hernandez-Hoyos, T. Sewell, R. Bader, J. Bannink, R.A. Chenault, M. Daugherty, M. Dasovich, H. Fang, R. Gottschalk, J. Kumer, R.E. Miller, P. Ravikumar, J. Wiens, P.A. Algate, D. Bienvenue, C.J. McMahan, S.K. Natarajan, J.A. Gross, J.W. Blankenship, MOR209/ES414, a novel bispecific antibody targeting PSMA for the treatment of metastatic castration-resistant prostate cancer, *Mol. Cancer Ther.* 15 (9) (2016) 2155–2165.
- [39] T. Ishiguro, Y. Sano, S.I. Komatsu, M. Kamata-Sakurai, A. Kaneko, Y. Kinoshita, H. Shiraiwa, Y. Azuma, T. Tsunenari, Y. Kayukawa, Y. Sonobe, N. Ono, K. Sakata, T. Fujii, Y. Miyazaki, M. Noguchi, M. Endo, A. Harada, W. Frings, E. Fujii, E. Nanba, A. Narita, A. Sakamoto, T. Wakabayashi, H. Konishi, H. Segawa, T. Igawa, T. Tsumihama, H. Mutoh, Y. Nishito, M. Takahashi, L. Stewart, E. ElGabry, Y. Kawabe, M. Ishigai, S. Chiba, M. Aoki, K. Hattori, J. Nezu, An anti-glypican 3/CD3 bispecific T cell-redirecting antibody for treatment of solid tumors, *Sci. Transl. Med.* 9 (410) (2017).
- [40] A. Seckinger, J.A. Delgado, S. Moser, L. Moreno, B. Neuber, A. Grab, S. Lipp, J. Merino, F. Prosper, M. Emde, C. Delon, M. Latzko, R. Gianotti, R. Luoend, R. Mur, R.J. Hosse, L.J. Harnisch, M. Bacac, T. Fauti, C. Klein, A. Zabaleta, J. Hillengass, E.A. Cavalcanti-Adam, A.D. Ho, M. Hundemer, J.F. San Miguel, K. Strein, P. Umama, D. Hose, B. Paiva, M.D. Vu, Target expression, generation, preclinical activity, and pharmacokinetics of the BCMA-T cell bispecific antibody EM801 for multiple myeloma treatment, *Cancer Cell* 31 (3) (2017) 396–410.
- [41] L.L. Sun, D. Ellerman, M. Mathieu, M. Hristopoulos, X. Chen, Y. Li, X. Yan, R. Clark, A. Reyes, E. Stefanich, E. Mai, J. Young, C. Johnson, M. Huseini, X. Wang, Y. Chen, P. Wang, H. Wang, N. Dybdal, Y.W. Chu, N. Chiorazzi, J.M. Scheer, T. Junttila, K. Totpal, M.S. Dennis, A.J. Ebens, Anti-CD20/CD3 T cell-dependent bispecific antibody for the treatment of B cell malignancies, *Sci. Transl. Med.* 7 (287) (2015) 287ra70.
- [42] K.L. Armour, M.R. Clark, A.G. Hadley, L.M. Williamson, Recombinant human IgG molecules lacking Fcγ<sub>2</sub> receptor I binding and monocyte triggering activities, *Eur. J. Immunol.* 29 (8) (1999) 2613–2624.
- [43] S.Y. Chu, I. Vostiar, S. Karki, G.L. Moore, G.A. Lazar, E. Pong, P.F. Joyce, D.E. Szymkowski, J.R. Desjarlais, Inhibition of B cell receptor-mediated activation of primary human B cells by coengagement of CD19 and Fcγ<sub>2</sub> with Fc-engineered antibodies, *Mol. Immunol.* 45 (15) (2008) 3926–3933.
- [44] S.J. Demarest, S.M. Glaser, Antibody therapeutics, antibody engineering, and the merits of protein stability, *Curr. Opin. Drug Discov. Devel.* 11 (5) (2008) 675–687.
- [45] S.R. Leong, S. Sukumaran, M. Hristopoulos, K. Totpal, S. Stainton, E. Lu, A. Wong, L. Tam, R. Newman, B.R. Vuilleminot, D. Ellerman, C. Gu, M. Mathieu, M.S. Dennis, A. Nguyen, B. Zheng, C. Zhang, G. Lee, Y.W. Chu, R.A. Prell, K. Lin, S.T. Laing, A.G. Polson, An anti-CD3/anti-CD19 bispecific antibody for the treatment of acute myeloid leukemia, *Blood* 129 (5) (2017) 609–618.
- [46] C. de Zafra, M. Balazs, F. Fajardo, L. Liang, W. Zhong, A. Henn, M.J. Bennett, G. Moore, U. Muchhal, D. Winters, B. Frank, K. Cook, J. Pearson, M. Melhem, V. Petrovic, R.J. Pelham, M. Friedrich, H. Tan, G. Moody, J. Stevens, J. Desjarlais, A. Coxon, O. Nolan-Stevaux, Preclinical characterization of AMG 424, a novel humanized T cell-recruiting bispecific anti-CD3/CD38 antibody, *Blood* 130 (2017) 500.
- [47] E.H. Sasso, G.J. Silverman, M. Mannik, Human IgM molecules that bind staphylococcal protein A contain VHIII H chains, *J. Immunol.* 142 (8) (1989) 2778–2783.
- [48] N.M. Stapleton, J.T. Andersen, A.M. Stemerding, S.P. Bjarnarson, R.C. Verheul, J. Gerritsen, Y. Zhao, M. Kleijer, I. Sandlie, M. de Haas, I. Jonsdottir, C.E. van der Schoot, G. Vidarsson, Competition for FcRn-mediated transport gives rise to short half-life of human IgG3 and offers therapeutic potential, *Nat. Commun.* 2 (2011) 599.
- [49] C. De Nardis, L.J.A. Hendriks, E. Poirier, T. Arvinte, P. Gros, A.B.H. Bakker, J. de Kruijff, A new approach for generating bispecific antibodies based on a common light chain format and the stable architecture of human immunoglobulin G1, *J. Biol. Chem.* 292 (35) (2017) 14706–14717.
- [50] S.Y. Chu, E. Pong, H. Chen, S. Phung, E.W. Chan, N.A. Endo, R. Rashid, C. Bonzon, I.W.L. Leung, U.S. Muchhal, G.L. Moore, M.J. Bennett, D.E. Szymkowski, J.R. Desjarlais, Immunotherapy with long-lived anti-CD123 × anti-CD3 bispecific antibodies stimulates potent T cell-mediated killing of human AML cell lines and of CD123+ cells in monkeys: a potential therapy for acute myelogenous leukemia, *Blood* 124 (2014) 2316.
- [51] S.Y. Chu, S.H. Lee, R. Rashid, H. Chen, E.W. Chan, S. Phung, E. Pong, N.A. Endo, Y. Miranda, C. Bonzon, I.W.L. Leung, U.S. Muchhal, G.L. Moore, M.J. Bennett, D.E. Szymkowski, J.R. Desjarlais, Immunotherapy with long-lived anti-CD20 × anti-CD3 bispecific antibodies stimulates potent T cell-mediated killing of human B cell lines and of circulating and lymphoid B cells in monkeys: a potential therapy for B cell lymphomas and leukemias, *Blood* 124 (2014) 3111.
- [52] S. Lee, S.Y. Chu, R. Rashid, S. Phung, I.W.L. Leung, U.S. Muchhal, G.L. Moore, M.J. Bennett, S. Schubert, C. Ardila, C. Bonzon, P. Foster, D.E. Szymkowski, J.R. Desjarlais, Anti-SSTR2 × anti-CD3 bispecific antibody induces potent killing of human tumor cells in vitro and in mice, and stimulates target dependent T cell activation in monkeys: a potential immunotherapy for neuroendocrine tumors, in: Proceedings of the 108th Annual Meeting of the American Association for Cancer Research 2017 April 1–5, Washington, DC (2017) Philadelphia (PA): AACR; 2017. Abstract nr 3633/6.
- [53] S.Y. Chu, Y. Miranda, S. Phung, H. Chen, R. Rashid, N.A. Endo, E.W. Chan, E. Pong, C. Bonzon, U.S. Muchhal, I.W.L. Leung, M.J. Bennett, G.L. Moore, D.E. Szymkowski, J.R. Desjarlais, Immunotherapy with long-lived anti-CD38 × anti-CD3 bispecific antibodies stimulates potent T cell-mediated killing of human myeloma cell lines and CD38+ cells in monkeys: a potential therapy for multiple myeloma, *Blood* 124 (2014) 4727.
- [54] M. Hedvat, M. Bennett, G. Moore, C. Bonzon, R. Rashid, S. Chu, K. Avery, A. Nisthal, U. Muchhal, J. Desjarlais, Dual blockade of PD1 and CTLA4 with bispecific antibody XmAb20717 promotes human T cell activation and proliferation, *J. Immunotherapy Cancer* 5 (Suppl 2) (2017) 87.
- [55] M. Hedvat, C. Bonzon, M.J. Bennett, G.L. Moore, K. Avery, R. Rashid, A. Nisthal, S. Schubert, R. Varma, S. Lee, L. Bogaert, I.W.L. Leung, S. Chu, U. Muchhal, J. Desjarlais, Simultaneous checkpoint-checkpoint or checkpoint-costimulatory receptor targeting with bispecific antibodies promotes enhanced human T cell activation, in: Proceedings of the 109th Annual Meeting of the American Association for Cancer Research 2018 April 14–18, Chicago, IL (2018) Philadelphia (PA): AACR; 2018. Abstract nr 2784/17.
- [56] G. Moore, M. Hedvat, M. Bennett, C. Bonzon, R. Varma, S. Schubert, S. Lee, K. Avery, R. Rashid, A. Nisthal, L. Bogaert, I. Leung, S. Chu, U. Muchhal, J. Desjarlais, Anti-PD1 × anti-ICOS bispecific antibody XmAb23104 brings together PD1 blockade and ICOS costimulation to promote human T cell activation and proliferation, *J. Immunotherapy Cancer* 5 (Suppl 2) (2017) 87.
- [57] M.J. Bennett, R. Varma, C. Bonzon, R. Rashid, L. Bogaert, K. Liu, S. Schubert, K.N. Avery, I.W.L. Leung, N. Rodriguez, S.Y. Chu, U.S. Muchhal, G.L. Moore, J.R. Desjarlais, Potency-reduced IL15/IL15Rα heterodimeric Fc-fusions display enhanced in vivo activity through increased exposure, in: Proceedings of the 109th Annual Meeting of the American Association for Cancer Research 2018 April 14–18, Chicago, IL (2018) Philadelphia (PA): AACR; 2018. Abstract nr 5565/21.
- [58] A.A. Zamyatnin, Protein volume in solution, *Prog. Biophys. Mol. Biol.* 24 (1972) 107–123.
- [59] M. Muda, A.W. Gross, J.P. Dawson, C. He, E. Kurosawa, R. Schweickhardt, M. Dugas, M. Soloviev, A. Bernhardt, D. Fischer, J.S. Wesolowski, C. Kelton, B. Neuteboom, B. Hock, Therapeutic assessment of SEED: a new engineered antibody platform designed to generate mono- and bispecific antibodies, *Protein Eng. Des. Sel.* 24 (5) (2011) 447–454.
- [60] A.F. Labrijn, J.I. Meesters, B.E. de Goeij, E.T. van den Bremer, J. Neijssen, M.D. van Kampen, K. Strumane, S. Verploegen, A. Kundu, M.J. Gramer, P.H. van Berkel, J.G. van de Winkel, J. Schuurman, P.W. Parren, Efficient generation of stable bispecific IgG1 by controlled Fab-arm exchange, *Proc. Natl. Acad. Sci. U. S. A.* 110 (13) (2013) 5145–5150.
- [61] T.S. Von Kreudenstein, E. Escobar-Cabrera, P.I. Lario, I. D'Angelo, K. Brault, J. Kelly, Y. Durocher, J. Baardsnes, R.J. Woods, M.H. Xie, P.A. Girod, M.D. Suits, M.J. Boulanger, D.K. Poon, G.Y. Ng, S.B. Dixit, Improving biophysical properties of a bispecific antibody scaffold to aid developability: quality by molecular design, *MAbs* 5 (5) (2013) 646–654.
- [62] H.J. Choi, Y.J. Kim, S. Lee, Y.S. Kim, A heterodimeric Fc-based bispecific antibody simultaneously targeting VEGFR-2 and Met exhibits potent antitumor activity, *Mol. Cancer Ther.* 12 (12) (2013) 2748–2759.
- [63] H.J. Choi, S.H. Seok, Y.J. Kim, M.D. Seo, Y.S. Kim, Crystal structures of immunoglobulin Fc heterodimers reveal the molecular basis for heterodimer formation, *Mol. Immunol.* 65 (2) (2015) 377–383.
- [64] H.J. Choi, Y.J. Kim, D.K. Choi, Y.S. Kim, Engineering of immunoglobulin Fc heterodimers using yeast surface-displayed combinatorial Fc library screening, *PLoS One* 10 (12) (2015) e0145349.
- [65] A. Leaver-Fay, K.J. Froning, S. Atwell, H. Aldaz, A. Pustilnik, F. Lu, F. Huang, R. Yuan, S. Hassanali, A.K. Chamberlain, J.R. Fitchett, S.J. Demarest, B. Kuhlman, Computationally designed bispecific antibodies using negative state repertoires, *Structure* 24 (4) (2016) 641–651.